The role of heat flux-temperature covariance in the evolution of weather systems

Marcheggiani and Ambaum

Author response to reviewers

We truly appreciate and are thankful for the effort that has been put by the Reviewers in reviewing our manuscript. Their comments are thoughtful and insightful and in responding to them we believe that the manuscript can benefit substantially. We hope that all their concerns have been duly addressed.

Reviewer's comments are reprinted in a *thinner and italicised style,* our response is typed below it in a thicker and non-italicised style.

Figures from the original manuscript are referred to following the manuscript's order while new figures included in this document are labelled as Figure AR# (Author Response).

Author response to Reviewer #1

We would like to thank Reviewer 1 for the detailed and insightful comments they gave on the manuscript, highlighting some unclear passages in the manuscript and highlighting studies on air—sea interaction which we did not discuss in our initial manuscript. Below we give a point-by-point response to the issues raised by the Reviewer.

One of the drawbacks of the paper concerns the physical meaning of the anomalies. The spatial variability of the sea surface temperature (SST) in the region near the Gulf Stream (GS) is generally due to the GS SST front. Here the spatial variability of the fluxes and temperature anomalies for timescales inferior to 10 days are not even presented. Is it related to the GS front? Centered over the front, or on its warm side? Is it related to oceanic eddies (as claimed near the end of the paper)? Understanding what are the characteristics of this variability is essential to the interpretation of the main results.

We believe there may have been some misunderstanding arising from our description of the mixed time-space anomalies. These are built as the spatial covariance of the departures from a 10-day running mean (which corresponds to a high-pass filter in the frequency domain), thus obtaining an instantaneous description of spatial patterns of synoptic-timescale variability (i.e. 10 days and below), which is what the paper is about. By removing a 10-day running mean, we are filtering out lower-frequency variability, such as seasonal variations, which may otherwise dominate the spatial variance, and which describes different physical processes.

We also emphasise that the high-pass time filtering occurs on the fluxes and the atmospheric temperatures, not on the SSTs. This means that the spatial variability caused by eddies on the gulf stream temperature front interacting with synoptic weather systems are in fact represented in our covariance index, and we show evidence that in the initial stage of development this is the key source of covariance.

We will rephrase the relevant passages in the manuscript to make this all more explicit and clear.

Another drawback is that a major process of air-sea interactions is completely overlooked: the so-called "oceanic baroclinic adjustment", as introduced by Nakamura et al. Their mechanism relies on the feedback of atmospheric temperature on air-sea fluxes. It seems to me that the results of the present manuscript are in disagreement with their findings. This issue should be tackled.

We are very thankful to the reviewer for highlighting the studies by Nakamura & co-authors on the role of the oceanic temperature front in storm track dynamics. In particular, they highlight the importance played by SST fronts in forcing a surface air temperature gradients through differential sensible heating across the SST front. This was shown to be essential for the maintenance of strong near-surface baroclinicity, which anchors the climatological storm track.

Our study does not contradict these results; in fact they are consistent with each other as well as complementary to each other. We find that the spatial variance of the fluxes, indeed including contributions of the N-S gradient of SSTs over the oceanic front, are associated with instantaneous depletion of baroclinicity. This is consistent with the mechanism discussed in a series of papers by Ambaum & co-workers highlighting the role that eddies play in temporarily depleting the baroclinicity in a predator—prey like relationship; this relationship is really a familiar instance of the nonlinear life-cycle of midlatitude eddies where meridional heat fluxes locally deplete the meridional temperature gradient in the atmosphere; in the older literature this quasi-periodic predator—prey relationship would have been described as an index cycle. However, this does not contradict the fact that high eddy activity on average must be geographically associated with high baroclinicity, which is essentially what the Nakamura papers are about, and of course also classical papers, such as Hoskins & Valdes (1990), and also Ambaum & Novak 2014.

So on a synoptic time-scale baroclinicity is depleted by synoptically induced variance of fluxes, as the many diagnostics in our manuscript show in various ways, but climatologically of course the storm track is anchored geographically by the high temperature gradients in the oceanic front, as highlighted by processes elucidated in the papers referred to by the reviewer, and in further detail in Swanson & Pierrehumbert 1997.

It is clear that this mutually complementary but consistent view on baroclinicity and spatial SST variance is an angle which we did not at all highlight in any detail in the manuscript, and we will discuss this in much greater detail in the revision.

A last drawback relies in the motivation of the paper, i.e. the study of the generation/depletion of available potential energy (APE) by air-sea fluxes. Surface fluxes are involved in the budget of temperature inside the boundary layer, not in the 850hPa temperature budget. Hence the product air-sea heat flux times 850hPa temperature (above the MABL) cannot be interpreted as a term related to APE production. It is more simply related to the relation of air-sea fluxes with the free troposphere.

We agree with the reviewer that our index is not formally equivalent to a term in the APE production budget —indeed, we never claimed as much— and we will rewrite the manuscript to make that clearer than we managed to do in the first version. We acknowledge that the hybrid framework we use can lead to confusion and we will rephrase in a clearer way the reasons behind its use in our study.

In our paper we work towards a hybrid understanding of how APE can be affected locally, in particular in response to coupling of the free troposphere with the surface. As the reviewer pointed out, the intensity and sign of surface heat fluxes are typically computed from the energy budget at the surface, hence their covariation with higher layers of the atmosphere is not trivial, and we believe it can have an effect on the evolution of weather systems.

More informally, we examine how synoptic heat fluxes contribute to enhancing or depleting the local synoptic variance in the lower tropospheric temperature field. This local temperature variance is of course part of the global APE integral in the standard Lorenz energy cycle.

1) I would have guessed that the variability of the air-sea fluxes lies above the warm side of the GS front, so that the spatial average used in (1) only captures this mode of variability. Indeed this *seems to be the case when looking at Fig.3. But, this would contradict line 257 where you say that spatial variability (at synoptic timescales) is due to mesoscale oceanic eddies.*

We look at the spatial covariance between heat flux and temperature time fluctuations from a centred ten-day average thus we expect part of the total variability over the Gulf Stream extension also to derive from the interaction between the atmosphere and colder waters. In particular, we surmised that the higher level of variability observed over the western end of the North Atlantic could be traced back to the presence of mesoscale oceanic eddies, which would provide for stronger spatial SST contrasts, and hence flux variance. In fact, in the eastern North Atlantic spatial variances and covariance between heat flux and temperature is much weaker (though we did not include this in the manuscript).

Here are some different questions:
- Can you provide some information about the variability of SST (e.g. std(SST'))?

SST time anomalies, defined as those used in the computation of the spatial covariance, would be much weaker than those for air temperature or heat fluxes as the former vary on much longer time scales. We point out again that we do not analyse the high-pass filtered SSTs, but the high-pass filtered fluxes. These contain the spatial variance introduced by the SST spatial variance, even if that had been chosen fixed in time.

The standard deviation in time of the SST is simply not a relevant diagnostic for pointing out a source of spatial variance in the synoptic time scale fluxes. A fixed SST front with no temporal standard deviation would still induce the spatial variance on synoptic time scales of the fluxes, which we diagnose. We will further emphasise this property in the revision to make this point clearer.

- Given the dataset you use (ERA-I at 1.5deg of resolution), you are unable to represent the small spatial scales present in the fields you examine. I would like that you redo Figure 3 with a higher resolution dataset (e.g. ERA-5 at 0.25deg) to see more clearly whether the SST front is important or not.

While it is true that ERA-I at 1.5°x1.5° resolution does not capture the smaller spatial scales, we found that using ERA-5 leads to slightly larger values for spatial covariance, as these smaller scales add to the variance. However, in the construction of composites, finer spatial details are lost due to the large number of events involved in the averaging process. Therefore, we believe the use of higher-resolution data proves most beneficial when looking at individual case studies.

- I do not see the point to show the SLP variance in Figure 1. Instead, could you present the std of F' and T' as well as the SST contours?

We agree that SLP variance is not the best choice in this context and we modified it accordingly (see Fig. AR1), thanks for pointing this out.

It is interesting to note that the peak flux standard deviation has a small bias towards the southern side of the SST front confirming a previous point by the Reviewer. This pattern is completely consistent with the mechanism of cold sector being advected in the SE direction over warmer (and spatially variable) SSTs.

- Lines 212-213, You present a scenario where a cold front moves above a spatially varying SST, which would trigger spatially varying heat fluxes and then spatially varying T850. But, in my opinion, the cold front is already associated with a strong T850 anomaly. Please explain why and how this anomaly will be enhanced (in particular at what spatial scales).

What is enhanced is the spatial variance of surface heat fluxes which is then followed in time by an increase in temperature spatial variance (we do not imply a causal link, which would act opposite). When the cold front moves across the spatial domain, the temperature spatial variance does not change significantly, while the surface heat fluxes pick up spatial variance when the cold sector moves over warmer SSTs. This is exactly the type of processes that our diagnostics highlight. Note also that this process is consistent with the new Figure 1 (Fig. AR1 in this response).

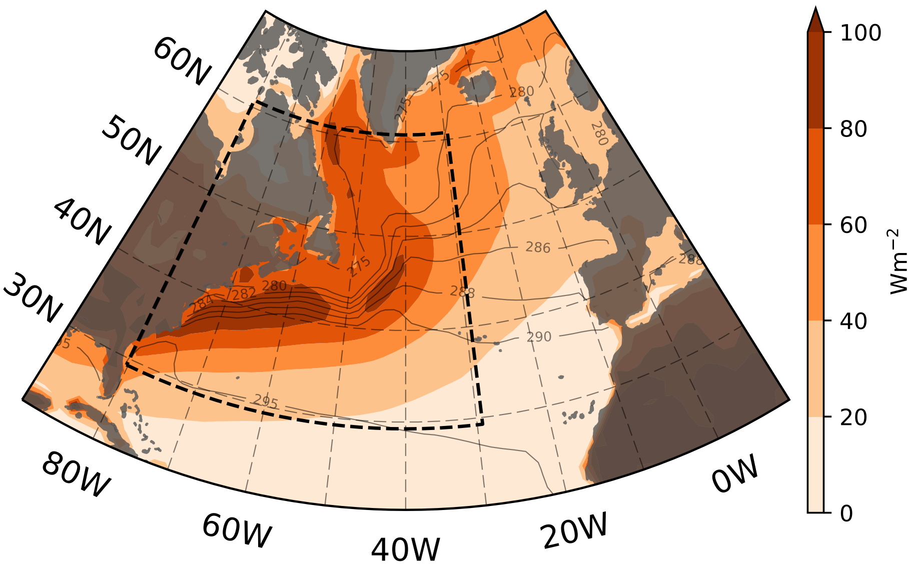

Figure AR1: Update of Figure 1 from manuscript; shading represents temporal standard deviation of F, contours represent SST winter climatology (every 2K from 280K to 290K, every 5K otherwise).

- Can you show a . of the time averages of [F' T'*] and [F' T'] to contrast in which spatial region the synoptic eddies give a different response to the total eddy field?*

The time average of either [F'*T'*] or [F'T'], assuming the brackets to be indicating a spatial average operator, would correspond to a negative number rather than a field. The time average of F'*T'* would instead provide a picture of where the spatial covariance of heat flux and temperature is realised within the spatial domain we considered. This is found to peak along the Gulf Stream, where time variances of the fluxes are also larger (see Fig. AR2 - and compare to Fig. AR1).

Thank you for pointing out this useful diagnostic; we will describe this property in the revision.

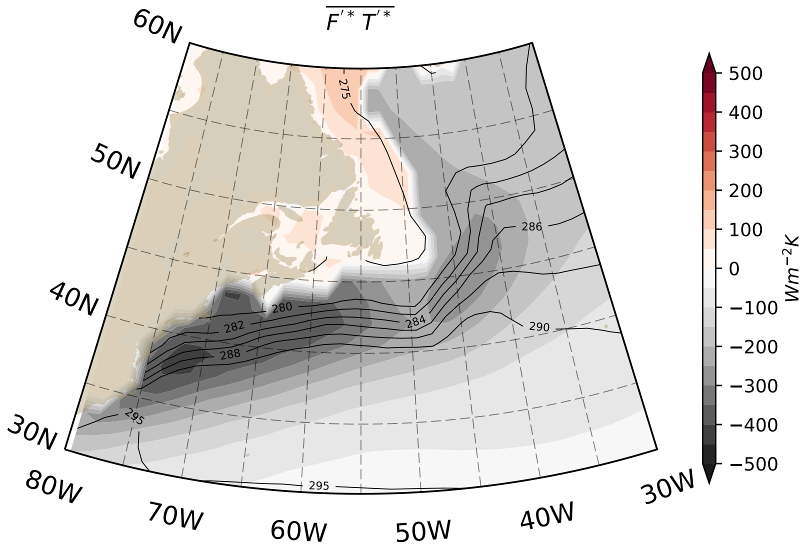

Figure AR2: Wintertime (DJF, 1979-2019) mean (shading) of product between time-space anomalies in flux and temperature over the spatial domain selected for our study. Black contours represent wintertime SST climatology (every 2K from 280K to 290K, every 5K otherwise).

2) You do not discuss at all of the mechanism proposed by H. Nakamura (Nakamura et al 2008 in GRL , Sampe et al. 2010 in J. Clim., Hotta and Nakamura 2011 in J. Clim), called the oceanic baroclinic adjustment (see Fig.12 in S10 or Fig. 20 in H&N11). This mechanism is related to a feedback between air-sea fluxes and surface temperature. Hotta and Nakamura relate the cold air advection of synoptic eddies to the interaction between air-sea temperature difference and air-sea fluxes. They stress the importance of SST gradient and surface baroclinicity. How does this relate to your Figure 4 and the co-evolution of T' and F'? More generally, please discuss their mechanism in comparison to yours.

We replied to this earlier and we agree that it will be a valuable addition to the manuscript to discuss the relation between these arguments and ours. As indicated before, we do not think they are contradictory at all; rather, they are complementary and really speak of different properties of the storm track.

3) I don't understand why you motivate your study by saying that FT is related to potential energy generation :
- Diabatic heating does not produce work, contrary to what is stated in line 2.

Thank you for pointing this out. That was indeed poorly phrased and will be changed. What we of course meant to say is that local diabatic heating and temperature anomaly fields need to be positively correlated for diabatic heating to maintain a circulation against dissipation.

- Surface fluxes are only involved in the budget of temperature inside the boundary layer (see for instance Small et al. 2013 in Clim. Dyn.). Hence the product air-sea heat flux times 850hPa temperature has no physical meaning, per se, and cannot be related to APE production, contrary to what is stated in lines 70-71.

- I don't understand why flux-temperature covariance affects baroclinicity (line 160), or APE generation (which is quite different from the former).

We are aware that the link we made between baroclinicity and available potential energy is informal and that direct expressions for local APE have been devised (Novak and Tailleux, 2017). As pointed out in an earlier response, we will put more effort in rephrasing clearly our intentions and the reasons why we have been using this particular framework.

4) I have some trouble to understand how you relate you covariance index to baroclinicity.
- Lines 158-159, you state that "baroclinicity was found to be depleted during extreme FT". However, from Fig.3b, it seems to me that baroclinicity is enhanced. Please explain.

Composites shown on the left in Figure 3 are relative to the peak in the covariance and we did not include lagged composites for the sake of conciseness. Perhaps it is useful to add composites at negative lags to illustrate more clearly how baroclinicity varies, as its depletion at larger FT covariance was indicated by phase tendencies presented in a later section.

In Fig. AR5 in this document it can be seen that the near surface temperature (T2m) at the peak does not particularly appear to coincide with an enhanced N—S temperature gradient. Furthermore, we produced a new Figure 3 (Fig. AR8 in this document) where it can be seen that the overall N—S gradient in T850 does not enhance at the peak of the index although local T850 gradients do appear to be somewhat enhanced, as suggested by the Reviewer. We will discuss this in the revision.

See also our response below.

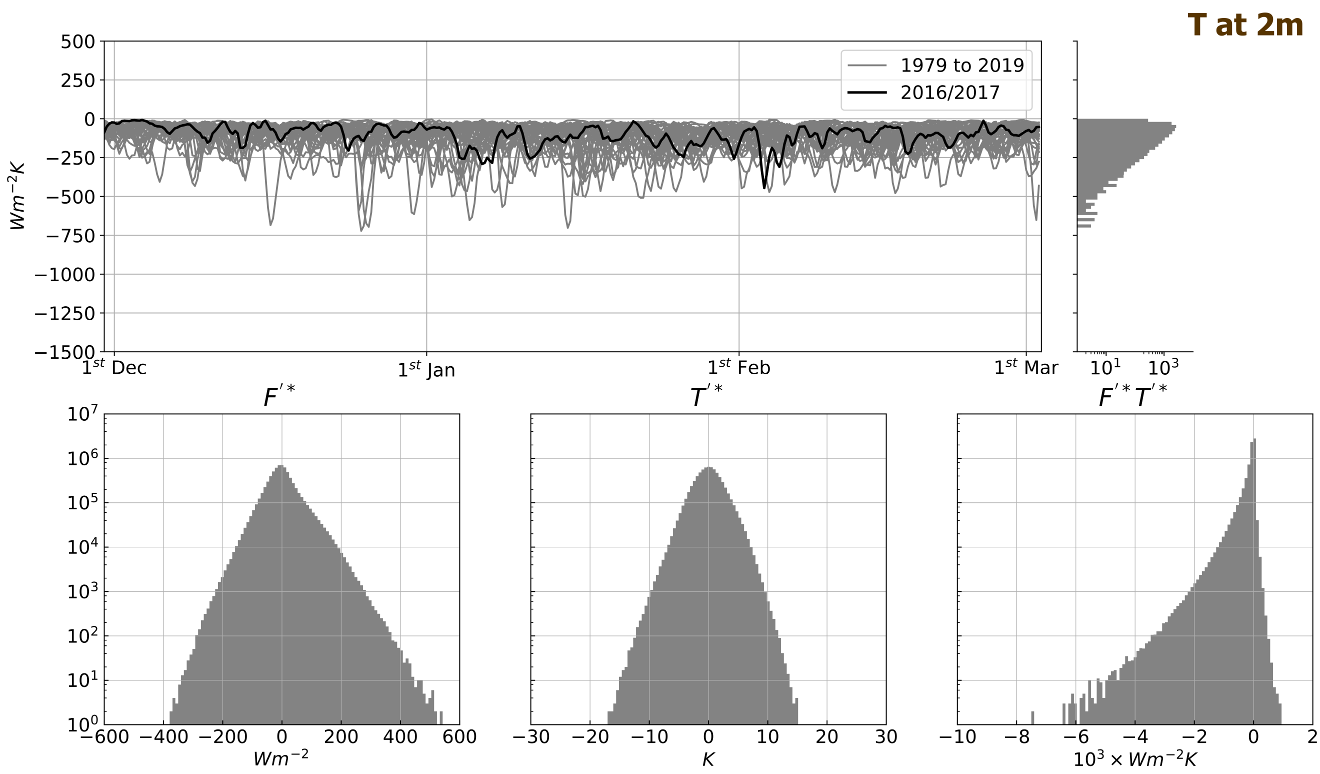

Figure AR3: As in Figure 2 of the manuscript using T2m as T.

- Also, you seem to relate mean baroclinicity (related to temperature gradients) and available potential energy (related to temperature anomalies), line 160. Please explain.
- Lines 252-253, you state that "air-sea exchanges drives the depletion of the baroclinicity over the domain". You seem to conclude this statement from the FT index life cycle which is not related to the baroclinicity.

Figure 4 in the manuscript really explains what we mean here: the baroclinicity is efficiently depleted following a peak in FT covariance. This is indicative of the two-way interaction between the two fields. We also see that when the FT covariance is weak, the baroclinicity can build up again. This is consistent with, for example, the set of papers of Nakamura et al., in that locally baroclinicity is produced over these regions, and it is consistent with the view that eddy activity locally (in time and space) depletes the temperature gradient.

The link between baroclinicity and APE has been investigated in previous studies such as Ambaum and Novak (2014). They also suggested the link between baroclinicity and local contributions to the APE in their study of storm tracks dynamics.

We realise that our discussion of these aspects should be clearer, and that we in particular did not include the relation to the climatological link between the SST front and the storm track. In the revised manuscript we will highlight those.

5) You seem to think that surface air temperature would not react as 850hPa temperature when computing covariances. Could you compute pdfs like Fig.2 using surface temperature (either 2m or 10m) instead of 850hPa temperature? From that point of view, I would also like that you add the 2m temperature and the SST in Figure 3.

Surface air temperature is directly involved in the computation of surface heat fluxes and this would just emphasise their strong interlink. Temperature at 850hPa, as the reviewer pointed out in a previous comment, is not directly involved in the computation of surface heat fluxes and therefore its covariation with surface heat fluxes is not trivial and entails more information

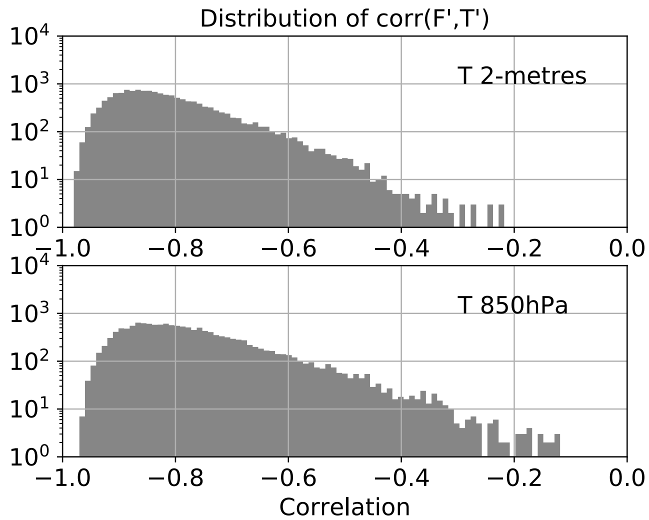

Figure AR4: empirical distributions of spatial correlation between F and temperature at the surface (top) and at the 850hPa level (bottom).

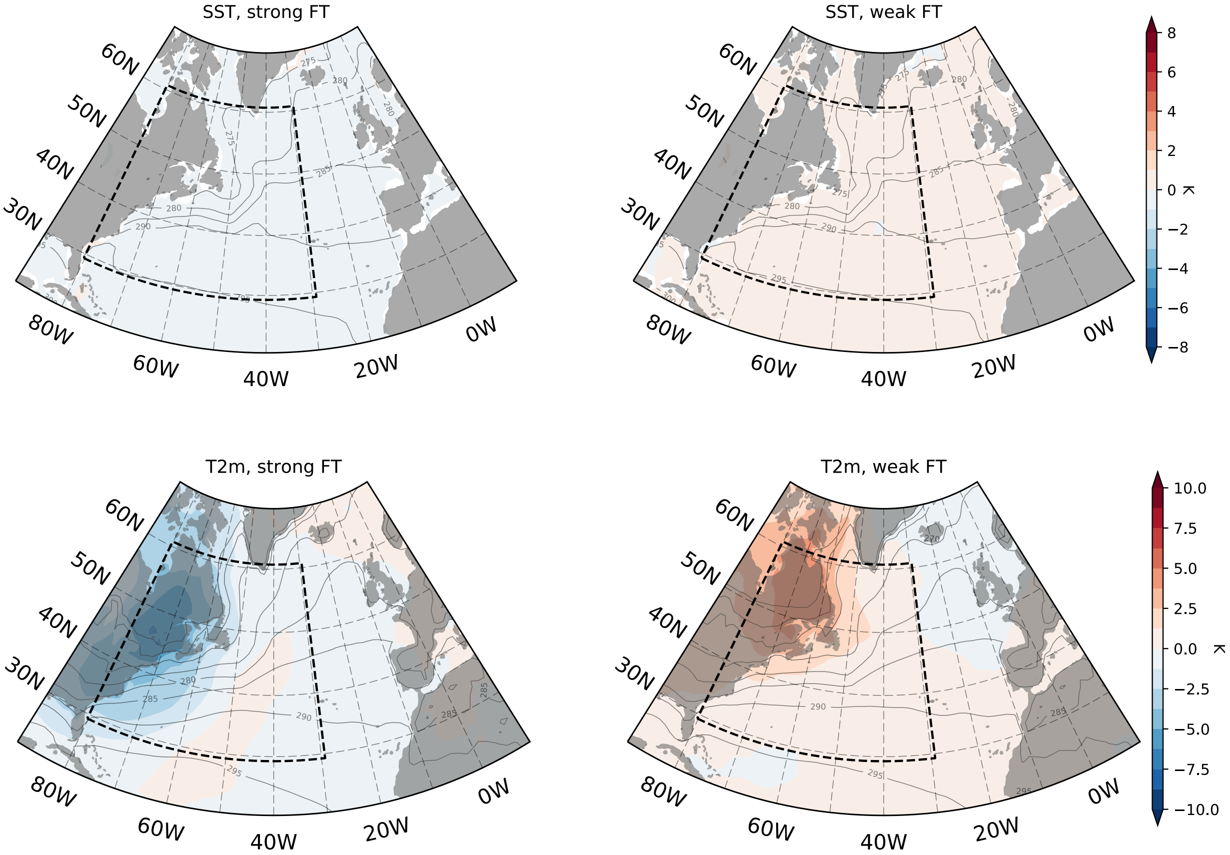

Figure AR5: As in Figure 3 for SST (top) and T2m (bottom) with contours representing the full composite and shading its deviation from climatology.

about synoptic developments, unlike temperature at the surface. The distributions using T at 2-metres are shown in Fig. AR3.

Covariances appear to be weaker when considering T2m which is due to the higher temperature variance at the 850hPa level. Indeed, the distribution for correlation between F and T2m is slightly shifted towards stronger values, while correlation between F and T850hPa features a longer tail towards weak values (see Fig. AR4).

The composites for SSTs (Fig. AR5, top) do not provide further insight into the coupling of the lower troposphere to the ocean surface on synoptic timescales, as these are much shorter than the typical time variability of SSTs.
Composites for T2m are remarkably similar to those for T850 (Fig. AR5, bottom), with slightly weaker anomalies' values (see Fig. AR7) and we will discuss this property in the revision.

5) The argument about the triggering for heat flux variability (line 265) would need more firm bases. Could you complement Figure 8b with time evolutions of sea level pressure and surface wind direction?

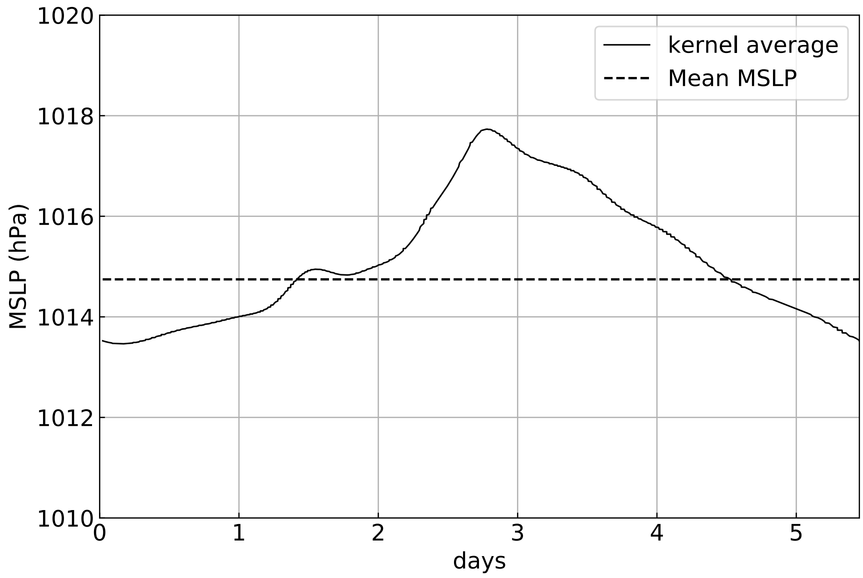

Figure AR6: Time evolution of kernel-averaged MSLP (solid line) and its climatological value (dotted line).

The time evolution of the average MSLP over the domain selected features a peak around day 3 of the path selected in Figure 8a, that is when FT spatial covariance is largest (see Fig. AR6).

The time evolution of the wind direction is shown in Fig. AR7 and is found to be consistent with cold air advection in the first half of the cycle and warm air advection in the second half.

We intend to add a discussion of these results in the revision and thank the Reviewer for suggesting this.

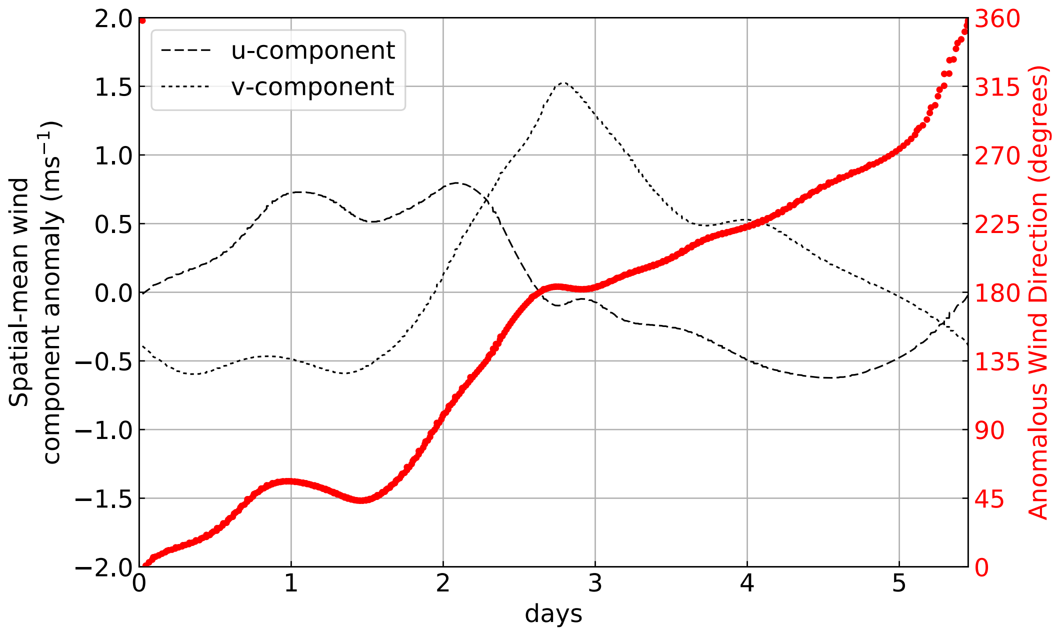

Figure AR7: Time evolution of meridional (dotted), zonal (dashed) anomalous wind components and corresponding anomalous wind direction (red dots).

6) The pdf file is really too big (40mb). It made my printer crashed. I urge you to produce a much smaller size pdf.

We apologise for this, it seems that the trouble is with Figure 6. The manuscript we submitted was only 8MB but printing it out would still give problems, as we just found out. We will make sure the reviewed manuscript prints out effortlessly.

— Minor points:
a) Figure 1 is too small when printed. Also, I don't understand why you chose to plot the SLP standard deviation. It would have been more logical to plot the T850 and the air sea-fluxes standard deviations (in blue and red) as well as the SST, since it is the subject of this paper.
b) Baroclinicity (line 154) should be defined.
c) Can you keep the spatial projections the same between figures: by choosing either the Conus representation (Fig.3) or the cylindrical one (Fig.1)

We will adjust figures according to both reviewers' suggestions.

Author response to Reviewer #2

1) The authors define the FT index by the spatial covariance between time anomalies in air-sea heat flux and 850 hPa temperature (equation 1). Why use both spatial and temporal deviations? Can the authors motivate this a bit better? How might an equation governing the APE, defined as both deviation from spatial and temporal mean, look like? The original definition by Lorenz is for spatial eddies (deviations from zonal mean). Later, Orlanski and Katzfey (1991) derived an alternative form for transient eddies (deviation from time mean). Perhaps the authors should provide reference for defining the APE as deviation from both time and spatial average? Defining the "energy" for a local region by subtracting the mean over that region is not necessarily useful due to the ambiguity of flux and conversion terms as Plumb (1983) pointed out.
References: Orlanski and Katzfey, 1991, JAS 48, 1972 Plumb, 1983, JAS 40, 1669

We acknowledge that the link we made between the APE budget and flux-temperature covariance is quite informal. Our intention was to capture the local air—sea heat exchange on synoptic time scales and elucidate their role in the evolution of a weather system. The seasonal progression of the meridional gradient would dominate over synoptic spatial variance, hence why we first remove a 10-day rolling average and then calculate the spatial anomalies. To that extent, we were not trying to obtain an expression for one of the various forms of APE.

I think the reviewer will also agree that there is no uniquely optimal choice of mean state or anomaly used to define APE, and no such thing as "the APE" exists. This is another reason why we used a more informal approach to defining a dynamically relevant thermodynamic index. Our index describes whether the air—sea heat fluxes locally act to increase or decrease synoptic variance in the lower-tropospheric temperature.

We are rephrasing the relevant passage as it also elicited questions from Reviewer 1 and it is then clear that our informal link to the APE budget was not made clear enough.

2) Related to the preceding point, to me, subtracting both the spatial and time mean makes it more difficult to visualize exactly how the passage of a system (e.g. a cold front) over the region would look like. Perhaps the authors should show figures corresponding to a time sequence of both the total fields and the eddy fields to make it easier for readers to understand some of the relationships found in this paper which seem to be a bit counter-intuitive.

We agree with the reviewer that showing the full fields as well as the mixed time-space anomalies could be helpful in understanding the role of flux-temperature spatial covariance in the evolution of a weather system. In fact, we did inspect these fields in more detail but decided to err on the side of not showing every possible field for the sake of brevity.

Nonetheless, we have decided to replot Figure 3 (see Fig. AR8) in order to include the full fields (contours) beside the anomalies (already shown as colour shading). We will use this figure in a revised manuscript, and include it here for inspection ahead of the revision.

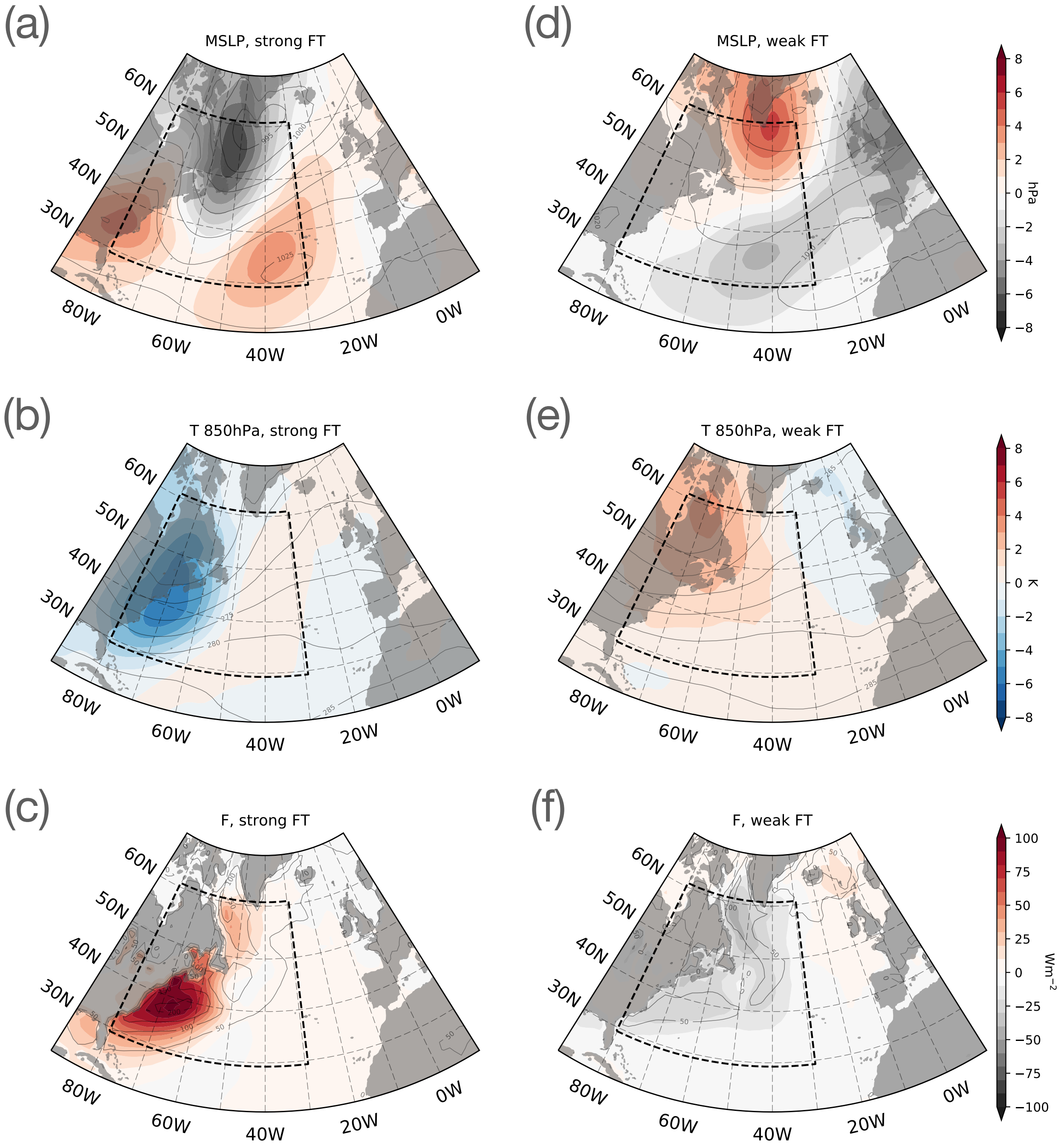

Figure AR8: contours indicate actual composite fields every 5 hPa, 5 K and 50Wm^{-2}, respectively for strong (a-c) and weak (d-f) FT index values.

3) A surprising result is that spatial variability in F' leads the spatial variability in T'. For weather systems of this time scale, one would expect that it is the atmospheric anomalies that force F', and thus it is, as the authors wrote, "counter-intuitive" (line 211). The authors explained that this "can be explained by the advection of the cold air mass, in the cold sector of a weather system, moving over a more spatially variable SST field such as that of the Gulf Stream extension. SST variability would trigger heat flux spatial variance which would then lead to temperature variance generation". I don't think I can understand this explanation. As the authors point out, F' nearly always damp T', and thus it is difficult to imagine how spatially varying flux, which acts to mostly damp the temperature anomaly, might give rise to increase in the temperature variance. Perhaps *the authors could show some sequence of snapshots along the phase space trajectory to show how this could happen and thus explain this "counter-intuitive" point better?*

Perhaps the term ‘lead’ in our description of the FT index dynamics can be misinterpreted. We literally meant “leading in time”, but did not want to imply any causal link. What we observed is that the increase in T’ spatial variance was followed by that in F’, which is the opposite of what would be expected if you interpreted F’ as a source of T’. But our work actually shows that the correlation is negative, indicating that T’ typically determines F’ (cold T’ leads to a positive F’ and v.v.) —with that causal link we might expect the T’ variance to lead the F’ variance but we actually find the opposite to be true, hence “counter-intuitive”.

We then surmised that this effect could be caused by the advection of cold air with a more spatially uniform temperature pattern over the Gulf Stream extension region, which features a much more variable temperature spatial field. The effect of surface heat fluxes would be that of eroding the spatial temperature variance in a weather system by damping the cold sector temperature anomaly, while the warm sector is less affected by this coupling with the surface.

Again, in the interest of compactness we decided to not show every possible diagnostic. We did select two relevant diagnostics in the paper which, as suggested by the reviewer, shows certain properties following the phase-space trajectory, namely the depth of the boundary layer (Figure 8) and the cold-sector area fraction (Figure 9). Figure 3 does not really show trajectories for synoptic fields but related composites, so they indicate the synoptic evolution. Nonetheless, kernel averages for strong and weak spatial standard deviations are able to reproduce the same spatial structures that are found by compositing on extreme values, as represented in Fig. AR9.

We are grateful for the reviewer for highlighting this aspect of our work, and in the revised version will include and reemphasise the above summary of the situation.

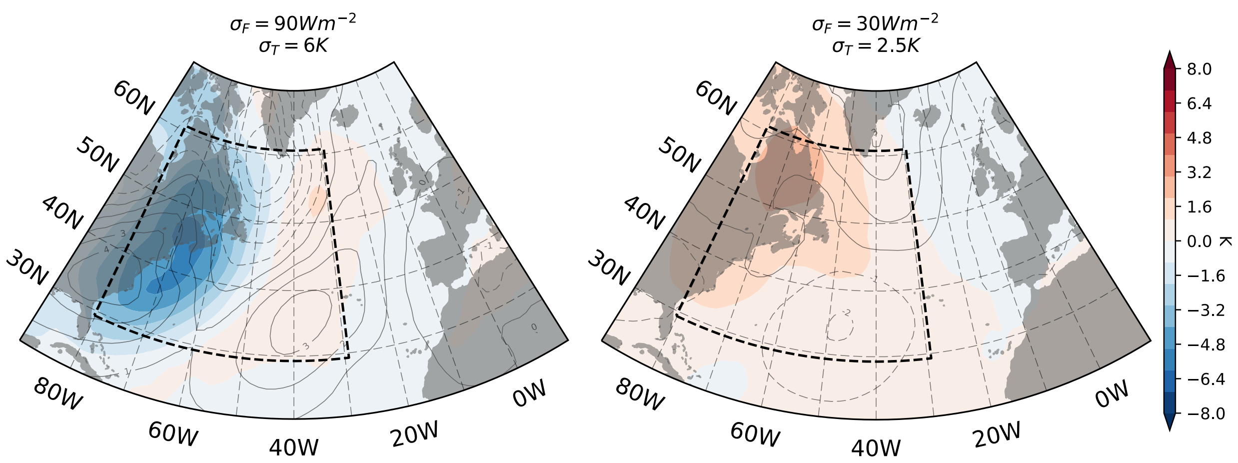

Figure AR9: kernel average of MSLP and T for strong (left) and weak (right) values of the spatial standard deviations in F’ and T’ (indicated at the top). Contours (every 1hPa, negative values dashed) and shading represent difference between kernel averages of MSLP and T and their winter climatologies, respectively.

Note also that in response to another Reviewer's query, we produced diagnostics of the wind direction and pressure following the phase space trajectory, analogous to Figure 8b in the manuscript (see Fig. AR7 in this document). As can be seen, the move towards the index peak (around "day 3") corresponds to a shift of the prevailing wind anomaly from initially N, N-W to W and then S at the peak, indicating an initial inflow from the cold sector into the domain going along with an enhancement of the system and the frontal winds.

4) One speculation about F' leading T'. F' reacts to surface temperature anomalies. The surface front leads the 850 hPa front by some time, could this lead to some time lag between F' and T'? Fig. 8b apparently shows upper level temperature anomalies leading lower tropospheric anomalies, but this is for the large scale baroclinic wave in which T anomalies tilt eastward with height (e.g. Holton's text book; Lim and Wallace 1991). The variance increase likely corresponds more to the propagation of the front rather than the large scale temperature anomaly associated with the baroclinic wave? Can the authors show that this is not the case?
Reference: Lim and Wallace 1991, JAS, 48, 1718

We certainly considered this interpretation of the tilt but initially thought that the tilt appeared insufficient to be consistent with such a baroclinic life cycle picture. We have now reconsidered some existing diagnostics, particularly from Lim & Wallace (1991), where a weak forward tilt of temperature is also diagnosed at lower levels, as it must be for growing waves (Hoskins & Heckley, 1981), but where it is also substantially less than the westward tilt of geopotential. Of course, the magnitude of the tilt is hard to compare to our results as the *x*-axis in our Figure 8 maps onto time in a non-trivial way.

The stronger tilt/lag of temperature at upper levels that we find is *not* consistent with observations or expected from theory of idealised life cycles, where in the lower stratosphere at least, the tilt/lag is expected to reverse, as suggested in the quoted studies.

Of course, as is the case with such diagnostic studies, it is not always obvious we are looking at growing, mature or decaying systems, even though we would expect dominance by the growing systems in the chosen geographical area.

So the question on whether the tilt is dynamically important remains open, and we are in fact currently working on a related problem. Our preliminary analysis shows that there may be contributions of non-normal growth as well as normal growth present in such statistics; of course the tilt of non-normal growth is not fixed and may potentially explain why the observed tilt in Figure 8 is so weak. This is however speculation at this point, and a topic in our current research.

Having reconsidered this issue following the Reviewer's suggestion, we conclude that this interpretation and discussion of the observed tilt is broadly consistent with our view of the synoptic development driving this index evolution, and we will want to discuss the above in the revision.

In particular, the temperature variance could well have been dominated by the cross-frontal temperature contrast being advected into the analysis area, while the flux variance is dominated by the cold-sector following the front. But if that were all there was to it, we would probably expect temperature variance to lead the flux variance, while we find the opposite to be true.

So it appears that the cold sector induced variance of fluxes shows up before the frontal temperature anomalies reach their maximum amplitude.

It is clear from the Reviewer's comment on this that this would be a valuable addition to the discussion and in the revised manuscript we will want to discuss this interpretation.

5) Lines 251-254: Increasing F' followed by decreasing baroclinicity does not really imply that baroclinicity is depleted by the air-sea exchange. Baroclinicity could be depleted by the growth of the baroclinic wave which occurs at the same time as the air-sea exchange is increasing. Causality cannot really be inferred when several things are occurring at about the same time, even with some slight lead-lag relationship.

The reviewer is of course right to stress the care that should be taken when inferring causality and we will emphasise that more in a revised manuscript.

Nonetheless, we believe from our analysis that there is strong evidence that the air—sea fluxes locally in time and space damp the synoptic temperature variance. From that point of view the interpretation that the FT index is a measure of both the eddy amplitude and how the air—sea fluxes might erode the eddy growth rate (baroclinicity) remains circumstantial but strong evidence.

We will caveat our discussion around Figure 4 to stress these important issues of interpretation.

6) Lines 59-61: There are "local" estimates using reanalysis data. For example, Chang et al (2002) showed that near surface sensible heat flux damps APE. See also Swanson and Pierrehumbert (1997) who also showed that 850 hPa temperature anomalies are strongly damped by surface fluxes over the ocean.
References: Chang, Lee, and Swanson, 2002: J. Climate, 15, 2163 Swanson and Pierrehumbert, 1997: JAS, 54, 1533

We are very thankful to the reviewer for highlighting the important links with these references. To our defence, we can only say that our route into this work came from a different direction —which we agree is a poor excuse! It is clear we will want to discuss the relevant links in a revised manuscript.

In particular, the importance of lower tropospheric thermal adjustment on short timescales to the underlying sea surface is something our work supports, and also supports the work that Reviewer 1 pointed out about the strong anchoring of the climatological storm-track to the ocean temperature front. In fact the inability to erode lower tropospheric temperature variance by synoptic eddies in the presence of strong SST variance is exactly consistent with our view that spatial variance in the SST is the cause of high flux variance which locally adjusts the lower tropospheric temperature by dragging it towards the SST. This happens at synoptic timescales.

7) Lines 270-272: As pointed out above, Chang et al (2002) showed that latent heating (formation of cloud and precipitation in the warm sector) does generate APE, but near surface sensible heating damps APE. They also showed that over the Atlantic, the net effect is damping in winter but there are some regions where there is net generation.

As indicated in our above answer, we are grateful to the Reviewer for highlighting this important link. We will revise that passage in order to take into account the study by Chang et al (2002) where they presented the contribution of the different components of diabatic heating to eddy APE. Their results are based on a dataset consisting of Januarys from 1980 to 1993 while we use the whole winter seasons from 1979 to 2019, though perhaps there are more recent studies with larger datasets that we are not aware of.

We did do many of our analyses using sensible heat fluxes as well as latent heat fluxes and total heat flux, and although the diagnostic results obviously differed in detail, and in magnitude, the structure of our main diagnostic results was quite insensitive to such choices. We did not endeavour and tease out the differences there were, as that would really constitute a different study. We decided to concentrate on sensible heat fluxes precisely because of the type of results presented in Chang et al., or Swanson & Pierrehumbert, as well as Hotta & Nakamura (2010), namely that sensible heat flux has a strong local effect of relaxing the lower troposphere towards the underlying sea surface.

8) In several places, the authors alleged to the importance of oceanic eddies (lines 91, 256, 258, 292). The data used is 1.5 degrees, and even the full resolution of ERA- Interim cannot really resolve oceanic eddies. If oceanic eddies are so important then how could the analysis based on ERA-Interim reveal that?

Although the spatial resolution we chose or even the finest available in ERA-Interim would not allow for oceanic eddies to be fully resolved, their effect on surface heat flux at the resolved scales would be captured by the reanalysis system which means there would be still some residual variance that can be revealed by our analysis, although obviously not all of it.

We are grateful for the Reviewer to point this out, as did Reviewer 1. We need to more acknowledge the potential role the overall N-S SST gradient could play in forcing variance in the fluxes; this contribution is obviously less sensitive the the underlying data resolution. Fig. AR1 in this document indicates how most of the flux variance (at least in time) is realised of the warmer part of the gulf stream front. This figure will replace the corresponding figure in the manuscript and we will duly discuss its properties and consequences.

9) The figures need to be improved. The legends are really small and can't be clearly seen without enlarging the figures by a lot.

We apologise to the Reviewer and agree to remake the plots to improve readability.

Minor comments:
i) Line 156: "lies almost entirely on the negative side of the FT index". I thought the FT index is always negative (line 97)?

That was badly phrased - apologies. Due to the kernel smoothing that was applied, in the phase plot it may seem that the index changes sign at times. However, the FT index is never positive, as stated earlier and also shown in Figure 2. We will make it clearer in the revised manuscript.

ii) Line 237: "A downward propagation of the temperature anomalies" - this is not really "propagation" - related to the eastward tilt of temperature with height in medium scale baroclinic waves discussed above.

Indeed. See also our response above.

The role of heat flux-temperature covariance in the evolution of weather systems

Andrea Marcheggiani[1] and Maarten H.P. Ambaum[1]

[1]Department of Meteorology, University of Reading, Reading, UK

Correspondence: Andrea Marcheggiani (a.marcheggiani@pgr.reading.ac.uk)

Abstract. Local diabatic heating and temperature anomaly fields need to be positively correlated for the diabatic heating to ~~produce work in the atmosphere~~maintain a circulation against dissipation. Here we quantify the thermodynamic contribution of local air–sea heat exchange on the evolution of weather systems using an index ~~for~~ of the spatial covariance between heat flux at the air-sea interface and air temperature at 850 hPa upstream of the North Atlantic storm track, ~~broadly~~ corresponding with the Gulf Stream extension region. The index is found to be almost exclusively negative, indicating that the air–sea heat fluxes locally act as a sink on potential energy. It features bursts of high activity alternating with longer periods of lower activity. The characteristics of these high index bursts are ~~studied~~ elucidated through composite analysis and the mechanisms are investigated in a phase space spanned by two different index components. It is found that the negative peaks in the index correspond with thermodynamic activity triggered by the passage of a weather system over a spatially variable sea-surface temperature field; our results indicate that most of this thermodynamically active heat exchange is realised within the cold sector of the weather systems.

1 Introduction

In the Northern Hemisphere, storm tracks are longitudinally localised, with the main regions of intense storm track activity ~~, both from an Eulerian (Blackmon et al., 1977) and a Lagrangian (Hoskins and Hodges, 2002) perspective,~~ located off the eastern coasts of mid-latitude Asia and North America. This is the case from a Eulerian (Blackmon et al., 1977) as well as a Lagrangian (Hoskins and Hodges, 2002) perspective.

Hoskins and Valdes (1990) emphasise the local Eady growth rate, the *baroclinicity*, as the dynamically relevant variable to determine the geographical structure of ~~the~~ storm tracks. Ambaum and Novak (2014) point out the ~~importance~~ relevance of baroclinicity in describing the temporal structure of storm tracks. They define a two-variable model which combines local baroclinicity and meridional eddy heat fluxes in a nonlinear oscillator and subsequently Novak et al. (2015) make use of it to explain regime transitions of the mid-latitude eddy-driven jet stream, which had been previously observed by Franzke et al. (2011). In particular, Novak et al. (2015) found that oscillations in baroclinicity and heat flux lead to variability in eddy anisotropy, which could then be associated with a major change in the dominant type of wave breaking (Hoskins et al., 1983), consequently affecting the jet stream latitudinal position, as is also observed in idealised experiments (Rivière, 2009; Orlanski, 2003).

Meridional heat fluxes can be interpreted as an indicator for the conversion of mean-flow to eddy available potential energy in the Lorenz energy cycle (Lorenz, 1955). Meridional and vertical heat fluxes act as conversion terms across different types of energy reservoirs, whereas surface heat fluxes are associated with generation and dissipation of available potential energy.

Global estimates of these terms have been computed (Peixoto and Oort, 1992) and were used to identify the direction of energy flow within the Lorenz energy cycle. Novak et al. (2017) demonstrate that the dynamical relationship between storm track intensity and available potential energy as measured by baroclinicity can be described by a ~~predator-prey~~ predator–prey relationship, whereby storm tracks can be thought of as *feeding* on baroclinicity.

The generation of eddy available potential energy ~~can be~~ in the Lorenz energy cycle is described analytically by a term which is proportional to the covariance between ~~surface heat flux~~ local heating and temperature (Lorenz, 1955; Peixoto and Oort, 1992; James, 1995). This term has been estimated to be positive globally (Oort, 1964; Oort and Peixoto, 1974; Ulbrich and Speth, 1991; Li et al., 2007; Marques et al., 2009), suggesting that diabatic processes are acting as a source of energy in storm development.

Diabatic processes at the surface, such as sensible and latent heat fluxes, ~~amplify the horizontal temperature gradient~~ can amplify horizontal temperature gradients by heating where it is warm and cooling where it is cold~~and thus generate~~, which is linked to the generation of available potential energy. From a global perspective this ~~can be~~ is achieved by the global differential in radiative ~~heating~~heat input. However, the local thermodynamic effects of latent and sensible heat fluxes are much less clear: upward air–sea heat fluxes typically may be expected to coincide with a cooler local atmosphere, suggesting a negative contribution to the local potential energy budget.

The importance played by sea surface temperature (SST) fronts in forcing surface air temperature gradients through differential sensible heating across the SST front has been highlighted in a series of studies (Nakamura et al., 2008; Hotta and Nakamura, 2011) . This mechanism, called *oceanic baroclinic adjustment*, was shown to be essential for the maintenance of strong near-surface baroclinicity, which anchors the climatological storm track.

Chang et al. (2002), using a dataset composed by Januaries from 1980 to 1993, described the contributions of the different components of diabatic heating to eddy available potential energy and showed that latent and sensible heating can have different effects on the potential energy budget. In particular, sensible heat flux was shown to have a strong local effect of relaxing the lower troposphere towards the underlying sea surface (Chang et al., 2002; Swanson and Pierrehumbert, 1997; Hotta and Nakamura, 2011) , while latent heating was not necessarily linked to local provision of heat input, because condensation may happen at a different location.

The intensity and sign of surface heat fluxes are typically computed from the near surface atmospheric conditions, hence their covariation with higher layers of the atmosphere is non-trivial and it can have an effect on the evolution of weather systems. The aim of this study is to identify and describe this local thermodynamic effect of air–sea heat fluxes. ~~In this framework, heat flux–temperature spatial covariance is considered~~

In particular, we examine how synoptic heat fluxes contribute to enhancing or depleting the local synoptic temperature variance in the lower troposphere. This local temperature variance is part of the global available potential energy integral in the standard Lorenz energy cycle. Therefore, we construct a hybrid framework where we can consider the spatial covariance between anomalous heat flux and temperature fields as a measure of the local contribution to diabatic generation or destruction of available potential energy~~and its evolution is linked to storm evolution~~ . We focus on the link with synoptic storm evolution by using time anomalies for all atmospheric fields as deviations from a synoptic-timescale mean.

This article is structured as follows: Section 2 briefly summarises the Lorenz energy cycle and the approach we take in our study. Section 3 introduces heat flux-temperature spatial covariance and examines its main features through the definition of an index. Section 4 investigates the driving mechanisms of the index previously introduced. Finally, in the final section results are summarised and discussed.

2 Lorenz Energy Cycle and flux–temperature covariance

Available potential energy can be generated globally through differential heating which amplifies ~~meridional temperature gradients~~ the global meridional temperature gradient and gives the troposphere in the mid-latitudes a baroclinic structure favourable to the growth of extra-tropical weather systems (Peixoto and Oort, 1992). In the Lorenz energy cycle (Lorenz, 1955) the interaction between different types of energy reservoirs is represented by conversion terms while surface heat exchange appears in energy generation and dissipation terms. Global estimates of these terms have been computed (Oort, 1964; Oort and Peixoto, 1974; Ulbrich and Speth, 1991; Li et al., 2007; Marques et al., 2009) and they are found to differ not only in time from seasonal to inter-annual scales, but also depending on the type of data variability considered, be it purely temporal, spatial or a combinations of these. For example, Oort (1964) found that generation of eddy available potential energy was negative in a spatial domain, whereas in a mixed space-time domain this was found to be positive. Ulbrich and Speth (1991) further decomposed eddy energy into stationary and transient components and estimated the former to be positive and the latter to be negative for January and July (averaged from 1980 to 1986) although with a difference in magnitude.

The generation and dissipation terms have normally been estimated as residuals in the main balance equations, as data for their direct computation typically were not archived. Global estimates normally suggest a positive generation of eddy available potential energy, which would involve heating of warm and cooling of cold air masses. ~~However,~~ Locally, however, model experiments with simplified climate models, where diabatic heating is ~~directly calculated~~determined as a relaxation of the temperature field, show a negative generation of eddy potential energy, with diabatic effects damping eddy available potential energy. This is also supported in studies by Swanson and Pierrehumbert (1997) and Chang et al. (2002), where they highlighted the importance of lower tropospheric thermal adjustment on short timescales to the underlying sea surface.

Given that storm tracks are by definition the main reservoirs of eddy potential energy, this begs the question of whether diabatic effects in storm tracks actually help or hinder their development, as investigated by Hoskins and Valdes (1990) who envisaged that sensible heating of cold air masses actually decreases the energy of weather systems while latent heating helps in their intensification in the warm sectors.

~~Here we~~ Given that there are different formulations of available potential energy budgets with each giving different interpretations from the same data, we will not favour any particular formulation here. Instead, we take a hybrid approach: we use direct estimates of ~~diabatic energy input~~ surface heat fluxes over the upstream sector of the North Atlantic storm track region and use

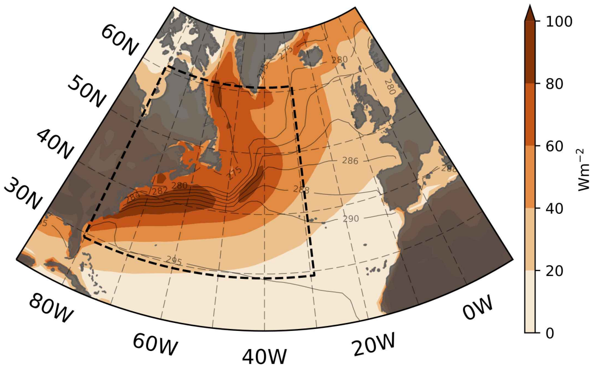

Figure 1. ~~Wintertime SSTs climatology~~ Temporal standard deviation of F (~~black contours~~shading) and ~~mean sea level pressure standard deviation in time~~ SST winter climatology (~~based on a 10-day running mean~~contours, every 2K from 280K to 290K, every 5K otherwise)~~;~~ ~~the~~. The area within the dashed box (30–60°N, 30–79.5°W) corresponds to the region of the N. Atlantic considered in the next sections for the computation of spatial averages.

it to estimate whether it ~~will~~ can serve as a source or as a sink of spatial variance in temperature. Available potential energy is a global ~~weighted integral~~ measure of such temperature variance. By defining a spatial covariance index between air–sea heat fluxes and lower atmospheric temperature we can quantify the extent to which the local heat fluxes help build available potential energy, or deplete it.

In particular, we consider the spatial covariance between time anomalies in instantaneous air–sea heat fluxes F' and air temperature T' at 850 hPa (see below) to define an area specific FT index,

$$\mathrm{FT} = \langle F'^{*} T'^{*} \rangle = \langle (F' - \langle F' \rangle)(T' - \langle T' \rangle) \rangle = \langle F'T' \rangle - \langle F' \rangle \langle T' \rangle, \quad (1)$$

where primes denote time anomalies~~with respect to a ten-day running mean~~, angle brackets spatial averages over the area selected and stars deviations from this spatial average. In order to concentrate on synoptic scale variability, time anomalies are defined as deviations from a running mean with a time window of 10 days (Athanasiadis and Ambaum, 2009). By removing a 10-day running mean in the construction of anomalies, we are filtering out lower-frequency variability, such as seasonal variations, which may otherwise dominate the spatial variance, and which describes different physical processes.

Data come from the European Centre for Medium-Range Weather Forecast (ECMWF) Re-Analysis Interim dataset (ERA-Interim, see Dee et al., 2011), restricting our attention to wintertime only (December to February, DJF), 6-hourly data from December 1979 to February 2019~~(~~, for a total of 40~~winters)~~ winters, interpolated onto a spatial grid with a resolution of 1.5° in both latitude and longitude. ~~In order to concentrate on synoptic scale variability, time anomalies are defined as deviations from a running mean with a time window of 10 days (Athanasiadis and Ambaum, 2009).~~ Instantaneous surface sensible heat fluxes have been utilised as a measure for heat exchange, F, which ~~is defined~~ we define as positive if heat flows upwards from the ocean to the atmosphere.

Repeating our analysis with latent heat fluxes or the sum of latent and sensible heat fluxes did not substantially change the outcomes we report on here, although values depending on heat flux magnitude of course change. The fact that the analysis seems mostly independent of which flux is used, indicates that the space and time filtered fluxes have a broadly fixed Bowen ratio on synoptic time scales.

The FT index was calculated over the western North Atlantic, extending between ~~30 – 60°N and 30 – 79.5°W~~30° – 60°N and 30° – 79.5°W, masking out land grid points in order to concentrate on air–sea interaction only. The domain selected is shown in Fig. 1 ~~, together with sea surface temperatures (SSTs) wintertime climatology and the time standard deviation of mean sea level pressure. The domain selected~~ and coincides with both the upstream region of the storm track ~~(region of stronger mean sea level pressure time variance)~~ and the Gulf Stream extension~~(strongest SST gradient)~~, where the largest SST variability is observed across different scales (e.g. large-scale meridional gradients and small-scale oceanic eddies). ~~Additionally, in the computation of the FT index land grid points are masked out in order to concentrate on air–sea interaction only~~Neither the spatial resolution chosen nor the finest resolution available in ERA-Interim would allow for oceanic eddies to be fully resolved. However, their effect on F at the resolved scales would be captured by the reanalysis system and they would still contribute some residual variance which is included in our analysis.

3 Temporal properties of the FT index

Figure 2 (top) shows the temporal behaviour of the FT index, Eq. 1, as defined for the upstream region of the North Atlantic storm track.

The index is found to be always negative and it features moderately frequent (strongest 5th percentile occurring once every 2–3 weeks) bursts of intense activity peaking at values down to almost $-1500\ \mathrm{Wm^{-2}K}$ among periods of weaker activity during which the index fluctuates around values closer to zero, although still keeping its negative sign. This ~~reflects on~~ is reflected in the empirical distribution of the index values, plotted to the right of the index time series in Fig. 2, featuring large skewness and an extended tail towards negative values, as well as a cut-ff for positive values.

The empirical distributions for the local values of F'^{*}, T'^{*} and $F'^{*}T'^{*}$ are shown in Fig. 2 (bottom left to right respectively). More than 9.5×10^6 data points across both the spatial and time domain were used, which allowed for the distributions in Fig. 2 to ~~result sufficiently smooth to~~ be examined without any sort of data filtering. These anomalies correspond to the anomalous fields constructed in order to calculate the index, which is the spatial average of $F'^{*}T'^{*}$.

The distribution for heat flux space-time anomalies is distinctively skewed towards negative values, whereas temperature anomalies follow more a Gaussian distribution. This is consistent with the different heat capacities of the atmosphere and the ocean, as the atmosphere is more easily heated by the ocean, while it takes both a longer time and a stronger vertical gradient in temperature for the atmosphere to flux heat into the ocean.

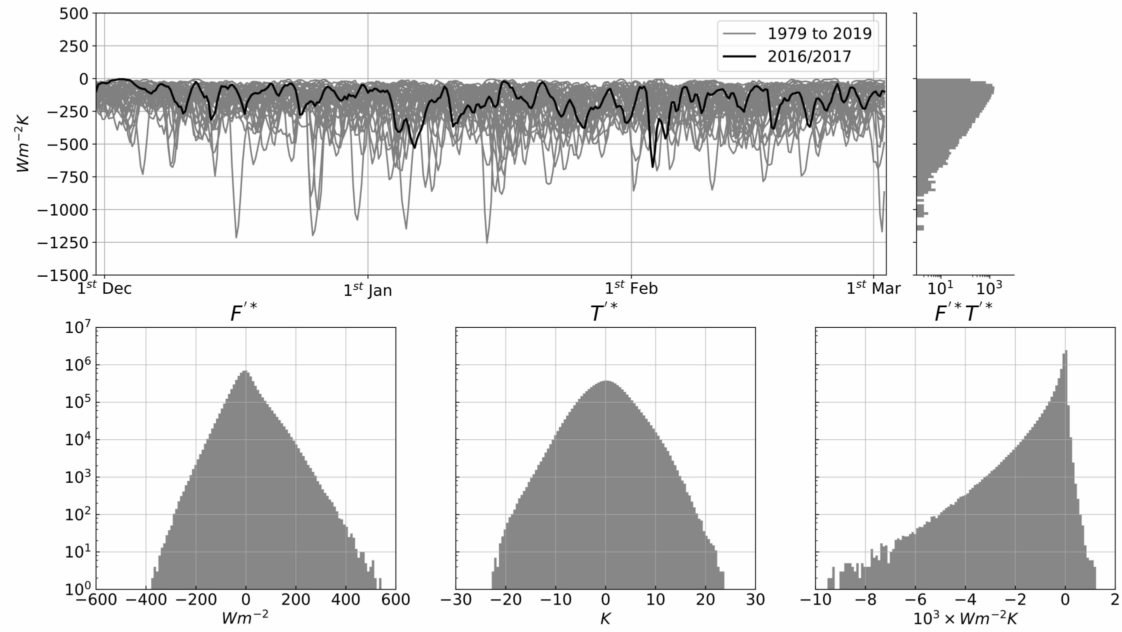

Figure 2. Top: Index time series computed over the upstream region of the N. Atlantic storm track (30–60°N, 30–79.5°W), spanning the full ERA-Interim time series (grey solid lines), highlighting a sample season (2016/2017 winter, solid black line); (right) empirical distribution of index values (semi-log scale). Bottom: Empirical distribution of instantaneous space-time anomalies in surface heat flux and temperature over the upstream region (semi-log scale).

The product of the local heat flux and temperature anomalies, on the other hand, shows an asymmetric distribution markedly skewed towards negative values with a long negative tail, indicating strong local negative correlation between the two variables. There are however a substantial number of positive values of the local product. These positive values correspond to heat flowing from an anomalously cold sea-surface to an anomalously warm air mass (and vice versa). The FT index is the spatial average of this signal and it is found to be always negative.

The local product is most often negative given that the air–sea heat fluxes are parameterised in terms of the temperature difference between the sea surface and the lower atmosphere. However, high instability in the lowest layers of the troposphere could cause the local product to become positive, as air temperature at 850 hPa is not directly used in the computation of surface heat fluxes. Furthermore, the transfer coefficient is a non-trivial function of boundary layer properties, not directly linked to the temperature at 850 hPa. It is therefore a non-trivial result that the FT index is observed to be negative at all times.

The sporadic nature of the strong negative index values suggest a link with weather system activity, as observed in for example in Messori and Czaja (2013a) and Ambaum and Novak (2014). Evidence for this link is shown in Fig. 3, where composites on the strongest and weakest FT index values are shown for mean sea level pressure, air temperature at 850 hPa and surface sensible heat flux. Strong FT index values (in the most negative 5th percentile) correspond to patterns associated with a low pressure system, with stronger than usual surface heat flux coinciding with cold air being advected from the American continent. Weak FT index (values in the top 5th percentile) correspond instead to inhibited storm activity, with weaker surface heat flux consistent with a pressure pattern which leads to weakened low level westerlies.

We chose T at 850 hPa as it is not directly involved in the computation of F and, therefore, its covariation with F is non-trivial and entails more information about development of the synoptic systems. Use of surface air temperature (T at 2-metre height) would serve to emphasise the strong interlink between temperature and surface heat fluxes, the computation of which directly involves T at the surface. In fact, covariances appear to be *weaker* when considering T at the surface, as temperature variance is higher at the 850 hPa level and, indeed, the distribution for correlation between F and T at the surface is slightly shifted towards stronger values, while correlation between F and T at 850 hPa features a longer tail towards weak values. Composites for T at the surface (not shown) are also found to be similar to those for T at 850 hPa (Fig. 3b,e) with slightly weaker anomaly values, which is likely caused by contribution from uncorrelated boundary layer dynamics in the production of temperature variance.

Lagged composites centred on extreme events were ~~computed (not shown)~~ also computed for mean sea level pressure, air temperature and precipitation rates, both convective and large-scale (as available from ERA-Interim, Dee et al., 2011), though not shown for the sake of conciseness. Between four and three days before the peak intensity in the FT index is reached, a low pressure system was observed entering the spatial domain, then intensifying at the FT index peak and finally decaying within synoptic time scales (three–four days).

~~Arguably, the~~ The intensification and decay phases observed in ~~lagged composites could be deriving~~ the lagged composites derives from a gain/loss of signal due to averaging of several different kinds of events, especially at longer lags. However, the decay phase was observed to be relatively rapid compared to the intensification phase, as weather patterns leading to the peak were observed to last longer than those ~~in the decay phase~~following the peak. This asymmetry between the initial and final stages of the FT index intensification is consistent with the idea that a strong negative FT index indicates a thermodynamic sink on the system.

~~Surface heat flux and temperature distributions are almost symmetric, centred on values relatively close to zero compared to extreme events in the tails, and feature weak skewness.The product of these anomalies, on the other hand, shows an asymmetric distribution markedly skewed towards negative values with a long negative tail, indicating strong local negative correlation between the two variables.~~

~~The FT index is the spatial average of this signal and it is never positive. Any positive index would correspond to heat flowing from an anomalously cold sea-surface to an anomalously warm air mass (and vice versa) which is less likely given that the air–sea heat fluxes are parameterised in terms of the temperature difference between the sea surface and the lower atmosphere.~~ The time average of $F'^{*}T'^{*}$, shown in Fig. 4, provides us with a picture of where the spatial covariance between F' and T' is realised within the spatial domain under consideration. This is found to peak along the Gulf Stream, where also the largest F time variance is observed (compare with Fig. 1), thus advocating for the importance of SST variability in shaping the $F' - T'$ spatial covariance.

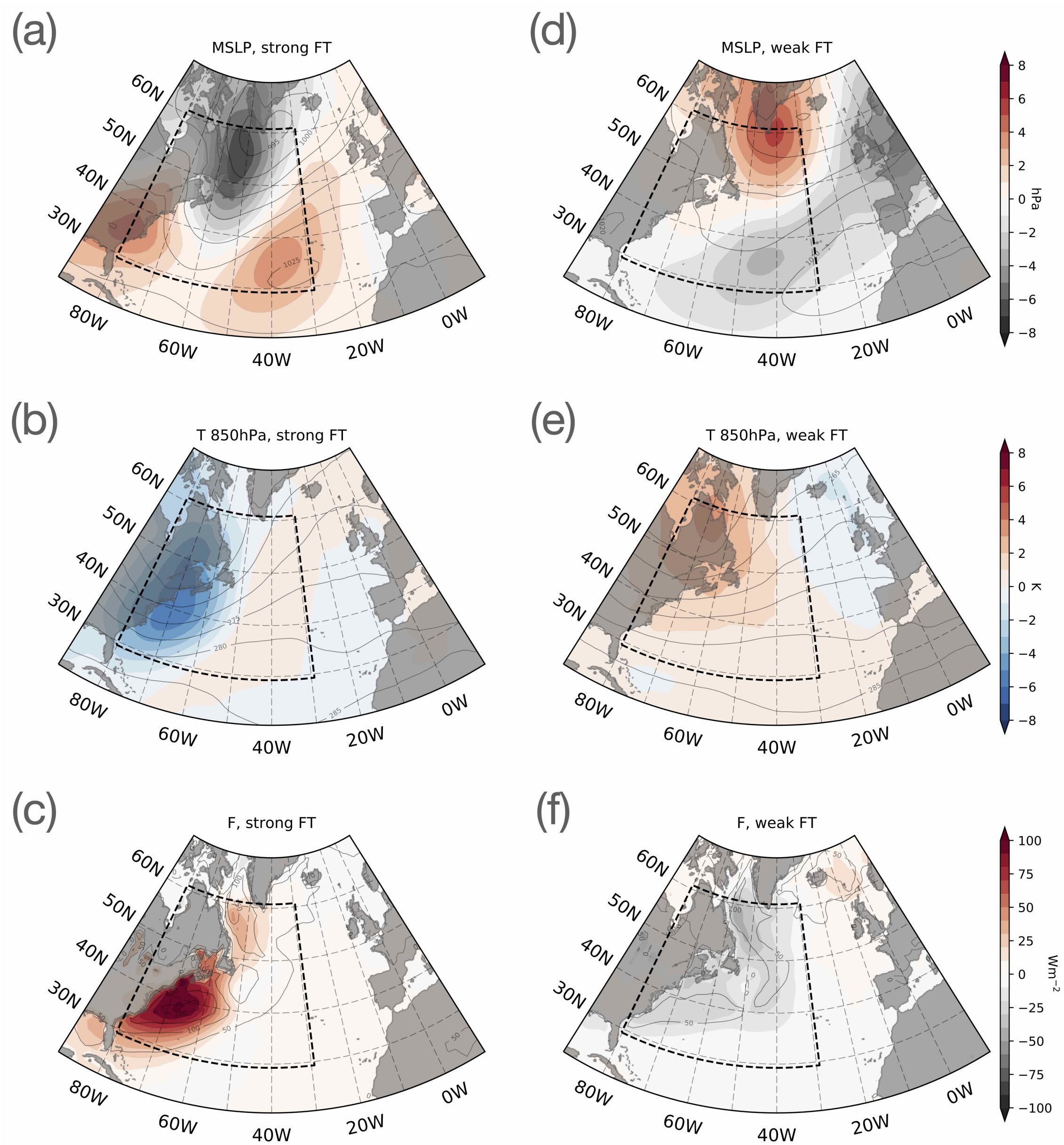

Figure 3. Composites on strongest (a–c) and weakest (d–f) FT index values (top and bottom 5th percentiles) for mean sea level pressure (a,d), air temperature at 850 hPa (b,e) and surface sensible heat flux (c,f). ~~Colour~~ Contours and colour shadings represent~~difference between~~ , respectively, composites and their difference from winter climatology; dashed boxes indicate the spatial domain where the FT index is defined.

~~However, high instability in the lowest layers of the troposphere could cause the index to become positive, as air temperature at 850 hPa is not directly used in the computation of surface heat fluxes.Furthermore, the transfer coefficient is a non-trivial~~

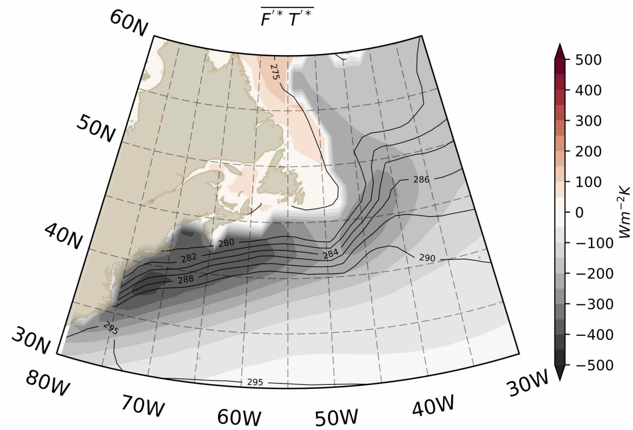

Figure 4. Wintertime (DJF, 1979-2019) mean of the product between time-space anomalies in F and T over the spatial domain selected for our study (shading) and wintertime SST climatology (contours, every 2K from 280K to 290K, every 5K otherwise).

~~function of boundary layer properties, not directly linked to the temperature at 850 hPa. It is therefore a non-trivial result that the FT index is observed to be negative at all times.~~

Note in addition that the FT index is ~~primarily~~ a measure of spatial variability and concurrent positive ~~(negative) anomalies in flux and temperature~~ or negative anomalies in F and T do not necessarily correspond to stronger ~~(weaker)~~ or weaker values compared to climatology~~, but would indicate stronger (weaker) ;~~,it would indicate a stronger or weaker intensity compared to both the surrounding area and the previous and following 5 days. We also found weaker negative FT index values to be indicative primarily of diminished storm activity, as Fig. 3 shows. Hence, it ~~seems~~ is reasonable to interpret any positive instances or moderately negative values as indicative of a relatively weak heat exchange, in the quiescent period between storm systems.

4 Phase-space properties of the FT index

We expect the FT index to be associated with variations in storm track properties. In order to get a clear picture of these associations we will employ a phase space kernel averaging technique.

The phase space is spanned by two variables. Any quantity can be kernel-averaged at any point in the phase space. We thus obtain a picture of how the quantity will depend on the two variables spanning the phase space.

A particularly interesting quantity to represent in such phase space is the tendency of the variables that span the phases space. In this way we can construct a flow in the phase space, representing the kernel averaged tendencies in the data.

The technical details of constructing the phase space averages and tendencies are described in (Novak et al., 2017)~~)~~. They constructed a two-dimensional phase space where they were able to identify a predator-prey relationship between meridional

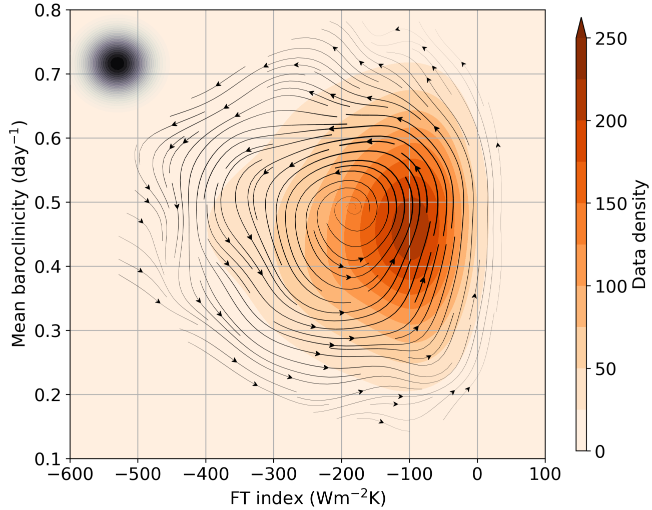

Figure 5. Kernel-averaged circulation in the FT index-mean baroclinicity phase space. Streamlines correspond to kernel-averaged rates of change in FT and baroclinicity (line thickness proportional to phase speed, plotted where data density is larger than 10). Colour shading represents kernel-smoothed data density. The size of the averaging Gaussian filter is indicated by the black-shaded dot in the upper-left corner.

heat fluxes and mean baroclinicity respectively, as these were used as coordinates in the phase space. Results may vary somewhat according to kernel size chosen, though in our study the results were observed to be broadly independent of the size of the kernel used for all reasonable size choices (not shown).

We start our analysis by constructing a phase space spanned by the FT index and ~~mean baroclinicityin~~ baroclinicity, measured as the Eady growth rate maximum (Hoskins and Valdes, 1990) spatially averaged across our chosen N. Atlantic storm track domain. The kernel averaged phase tendencies for the FT index and mean baroclinicity are shown in Fig. 5.

We find that the circulation in the FT–baroclinicity phase space lies ~~almost~~ entirely on the negative side of the FT index axis and it is in the anti-clockwise direction. ~~Furthermore, it can be observed~~ (The few trajectories crossing into the positive FT index region are due to kernel smoothing.) The phase portrait indicates that mean baroclinicity ~~is~~ becomes depleted when the FT index is strengthening and it recovers only at lower FT~~index values. This~~ index values, which is consistent with results of composite analysis, ~~as~~ whereby baroclinicity was found to ~~be depleted~~ reduce during extreme events in the FT~~index.~~ index (not shown). The observed baroclinicity depletion could be linked to the growth of baroclinic waves happening at the same time as the FT index increases, therefore care should be taken in inferring causality. Nonetheless, our analysis is consistent with the picture that air–sea fluxes locally in time and space damp the synoptic temperature variance, as the negative FT index acts as a measure of both eddy amplitude and of how air–sea heat fluxes might erode temperature gradients (i.e. baroclinicity).

~~This~~ These results do not contradict the findings by Hotta and Nakamura (2011) and are actually complementary to them. In fact, the spatial variance of the fluxes includes contributions also from the north-south gradient of SSTs over the oceanic front. This is consistent with the mechanism discussed in Ambaum and Novak (2014); Novak et al. (2017) where the authors highlight the role that eddies play in temporarily depleting the baroclinicity in a predator–prey like relationship. This relationship is really an instance of the nonlinear life-cycle of midlatitude eddies where eddy activity locally depletes the meridional temperature gradient in the atmosphere. (In the older literature this quasi-periodic predator–prey relationship would have been described as an index cycle.) However, this does not contradict the fact that high eddy activity on average must be geographically associated with high baroclinicity, as argued by Hotta and Nakamura (2011), Ambaum and Novak (2014) and elucidated also in earlier studies by Swanson and Pierrehumbert (1997) and Hoskins and Valdes (1990).

Our analysis suggests that the flux-temperature spatial covariance plays an important role in the budget for mean baroclinicity ~~(and~~and, more generally, for available potential energy ~~, more generally) and any mechanism driving~~ (Ambaum and Novak, 2014), alluding to the existence of a link between any driving mechanism behind the FT index ~~should be linked to~~ and storm evolution.

In fact, ~~this result suggest~~ our result shows that the FT index is a good measure of processes that deplete baroclinicity.

~~Kernel-averaged circulation in the FT index-mean baroclinicity phase space. Streamlines correspond to kernel-averaged rates of change in FT and baroclinicity (line thickness proportional to phase speed, plotted where data density is larger than 10). Shading represents kernel-smoothed data density.~~

The FT index can be decomposed into the product of flux-temperature spatial correlation and spatial standard deviations in flux and temperature,

$$\text{FT index} = \text{cov}(F', T') \equiv \text{corr}(F', T')\,\sigma(F')\,\sigma(T'). \tag{2}$$

This suggests we can also use spatial standard deviations in ~~F and T~~ F' and T' as coordinates of the phase space where trajectories traced by the index components would represent its evolution across the various components of the index.

The occurrence of strong index values can be explained by increasing variance in either heat flux or temperature, or anomalously strong correlations between the two variables. Another possibility is of course that a combination of any of these three factors produces strong index events.

This question of magnitude driven or phase driven index extremes is ~~similar~~ analogous to that presented in Messori and Czaja (2013b) for meridional heat transport ~~although we use a different approach to determine which case is closest to reality through phase tendencies analysis~~ and our phase space analysis provides a novel viewpoint of the phenomenon.

Figure 6a shows the ~~picture resulting~~ result from kernel-averaging in ~~our~~ a phase space spanned by the variances in heat flux and air temperature. Here streamlines indicate the phase space mean trajectories and their thickness is proportional to the phase speed, while the shading represents the typical value of the FT index at each point in the phase space as resulting from kernel-averaging~~, i. e. its phase tendency.~~.

Regions in the phase space where data is scarce (less than 10 and 1 data points respectively for streamlines and ~~phase tendencies~~FT index value) are hidden as kernel-averages there are not representative of the local value of the variable.

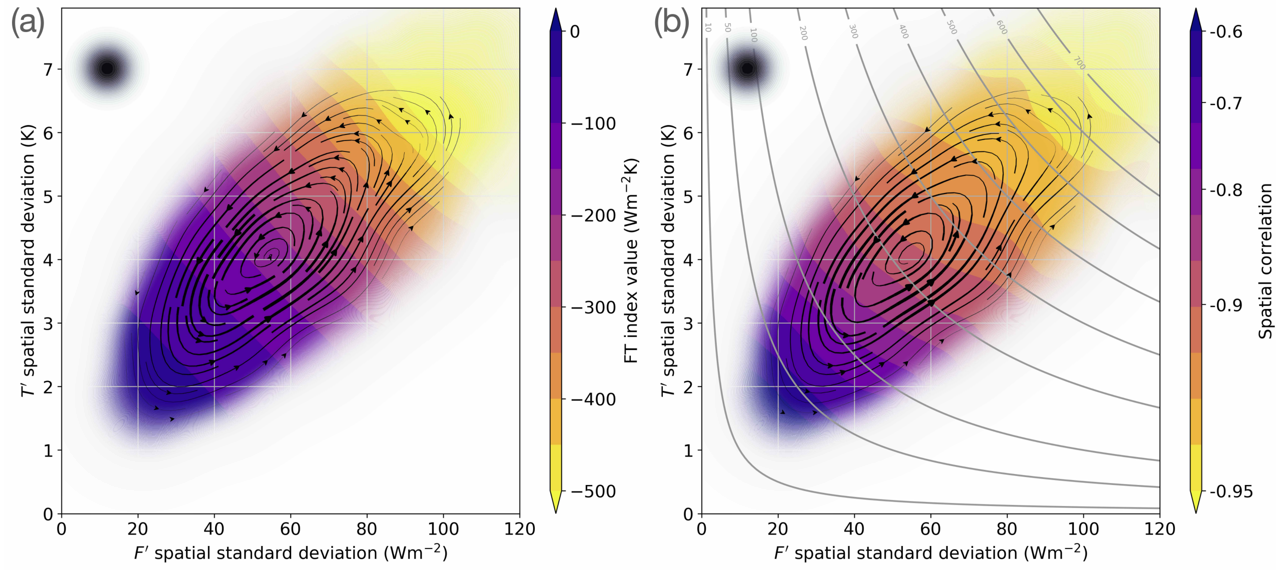

Figure 6. Kernel-averaged circulation in the F'-T' spatial standard deviations phase space. Streamlines correspond with kernel-averaged trajectories traced by the product of spatial standard deviations (line thickness proportional to phase speed, plotted where data density is larger than 10). Shading represent ~~phase tendencies for~~ values of the FT index value (panel a) and FT spatial correlation ~~in panels (a) and (~~panel b)~~respectively~~. Grey contours in panel (b), drawn at 10 $\mathrm{Wm}^{-2}\mathrm{K}$, 50 $\mathrm{Wm}^{-2}\mathrm{K}$, 100 $\mathrm{Wm}^{-2}\mathrm{K}$ and then every 100 $\mathrm{Wm}^{-2}\mathrm{K}$, indicate the product of spatial standard deviations. The size of the averaging Gaussian filter is indicated by the black-shaded dot in the upper-left corner.

The trajectories traced by the FT index components are found, on average, to be oscillating between low and high values of the index, which is consistent with the behaviour observed in the time series and shows that stronger index values are associated with larger variances in F' and T'.

The trajectories are also observed to be oscillating between weak and strong F'-T' spatial correlation, as shown by spatial correlation phase tendencies illustrated in Fig. 6b.

Taking a closer look at the relationship between spatial correlation and standard deviations in F' and T', these appear to be growing concurrently. This can be deduced by inspecting Fig. 6b, as spatial correlation is observed to increase together with the product of spatial standard deviations in F' and T', which is represented by grey contours.

In Fig. 7, spatial correlation is plotted against the product of standard deviations in F' and T' using values from ~~the phase tendency in~~ Fig. 6b (dark-grey dots) and then compared with raw data (light-grey dots) in order to exclude it being an artefact of kernel-averaging. Spatial correlation and variances are found to be in an almost log-linear relationship, with ~~phase tendencies~~

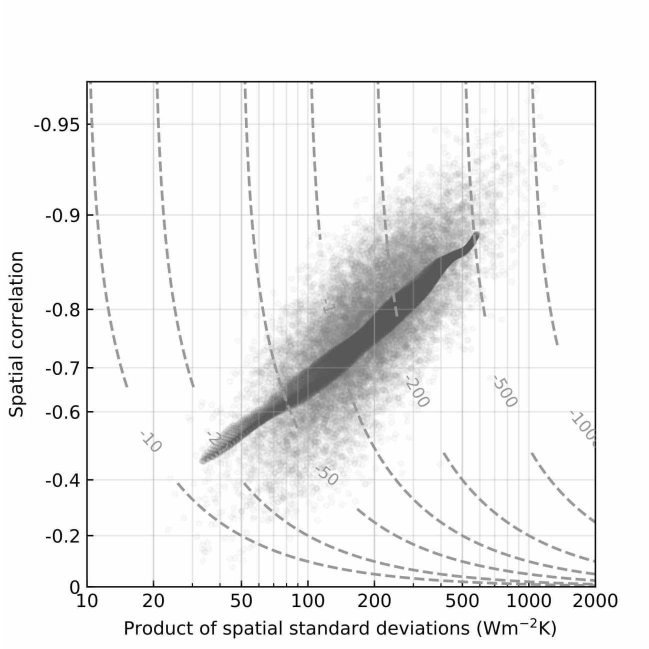

Figure 7. Scatter plot of F'-T' spatial correlation against the product of F' and T' standard deviations using kernel-averaged data points from phase portrait (dark shading) and raw data (grey dots); grey contours ($\mathrm{Wm}^{-2}\mathrm{K}$) indicate FT index value.

~~indicating increases in correlation as~~ both phase space data and raw data indicating an increase in correlation strongly linked to ~~increases in variances, while raw data point perhaps to an even stronger link~~an increase in variances.

These results suggest that the observed bursts in flux-temperature spatial covariance are neither exclusively phase-driven nor exclusively magnitude-driven. Both high flux and air temperature spatial variability and correlation are characteristic features of the bursts. We conclude that both strength and correlation in spatial variability are equally fundamental to the build up of flux-temperature spatial covariance.

It is not clear why the correlation between the two variables increases so markedly with their variability. The simple model of flux being essentially proportional to the temperature at 850 hPa (minus the SST) would not exhibit such a behaviour.

The simultaneous growth of correlation and variance is a non-trivial result and it suggests further research into assessing whether this is a general feature of the relationship between flux and lower atmospheric temperature or if it is limited to spatial variability dynamics or to the specific timescales considered. This would go beyond the scope of the present paper, but preliminary analysis indicates that the increase of correlation with variance may be a more generic property of the relationship between air–sea flux and lower atmosphere temperature.

The kernel-averaged trajectories in the phase space are organised in concentric ellipses, which suggests that the evolution of the FT index is cyclical in nature. By computing the average phase speed at which the trajectories are traced, it is estimated that it takes between 4 and 6 days for the FT index to go round a full cycle (see Fig. 10a for a sample trajectory). This time frame (4-6 days) falls within the range of synoptic timescales, consistently with the idea that the index is closely linked to the evolution of a storm system.

We then notice that the observed circulation spins in an anticlockwise direction. This indicates that the spatial variability in F' leads in time on the spatial variability in T', as can be seen by following any of the trajectories starting from weak index values.

This ~~may be~~ is somewhat counter-intuitive~~, but can be explained~~ . A possible explanation is that this effect could be caused by the advection of ~~the cold air mass, in the cold sector of a weather system, moving over a more spatially variable SST field such as that of~~ cold air with a more spatially uniform temperature pattern over the Gulf Stream extension ~~. SST variability would~~ region, which features a much more spatially variable temperature field. SST spatial variability would then trigger heat flux spatial variance ~~which would then~~ and subsequently lead to temperature variance generation.

~~The~~ In the case of a weather system, the effect of surface heat fluxes would be that of eroding the spatial temperature variance by damping the cold sector temperature anomaly, while the warm sector is less affected by this coupling with the surface. Kernel averages for strong and weak spatial standard deviations in F' and T' (not shown) were found to be able to reproduce the same spatial structures that are found by compositing on extreme values (Fig. 3), which further supports the idea of the cold sector playing a primary role in the evolution of the FT index~~is further supported by the study of phase tendencies in~~ .

Further evidence to the importance of the cold sector is gathered by inspecting phase tendencies of F and T.

Figure 8 shows phase tendencies for spatial-mean heat flux F and air temperature T. We find that the growing phase of the FT index coincides with a decrease in mean T and a concomitant increase in mean F. A decay phase then follows, characterised by the opposite trends.

Heat flux anomalies range from $-20\ \mathrm{Wm^{-2}K}$ in the decay phase up to $40\ \mathrm{Wm^{-2}K}$ in the growing phase, while air temperature anomalies stretch between -2 K and 2 K respectively. The standard deviations in time of spatial-mean F and T are respectively $23.3\ \mathrm{Wm^{-2}K}$ and 2.2 K, suggesting that these signals do not arise exclusively from random fluctuations and thus providing our results with robustness.

Phase tendencies in Fig. 8 may be explained by relating the growing and decaying phases to an increased dominance of the cold sector of weather systems in the former, while the warm sector influences the latter. This would be in agreement with composite analyses for convective precipitation (not shown), which showed a precipitation band coinciding with the cold front as identifiable from the air temperature composite.

Further evidence to the importance of the cold and warm sectors in the evolution of the FT index ~~is found as follows~~can be found in a more detailed analysis of the index dynamics in the phase space. A closed trajectory in the phase space is chosen by selecting a line of constant value of the stream function which was computed to draw the streamlines shown in the phase portraits. The selected closed trajectory is illustrated in Fig. 9 and a complete revolution takes about 5 days. It crosses regions of high data density so that it corresponds to a ~~larger~~ large number of unfiltered trajectories (i.e. not kernel-averaged) ~~thus more likely to be representative of real events rather than just of a mean behaviour~~and thus presents a statistically robust picture.

~~Figure 10b shows the difference between the kernel-averaged~~

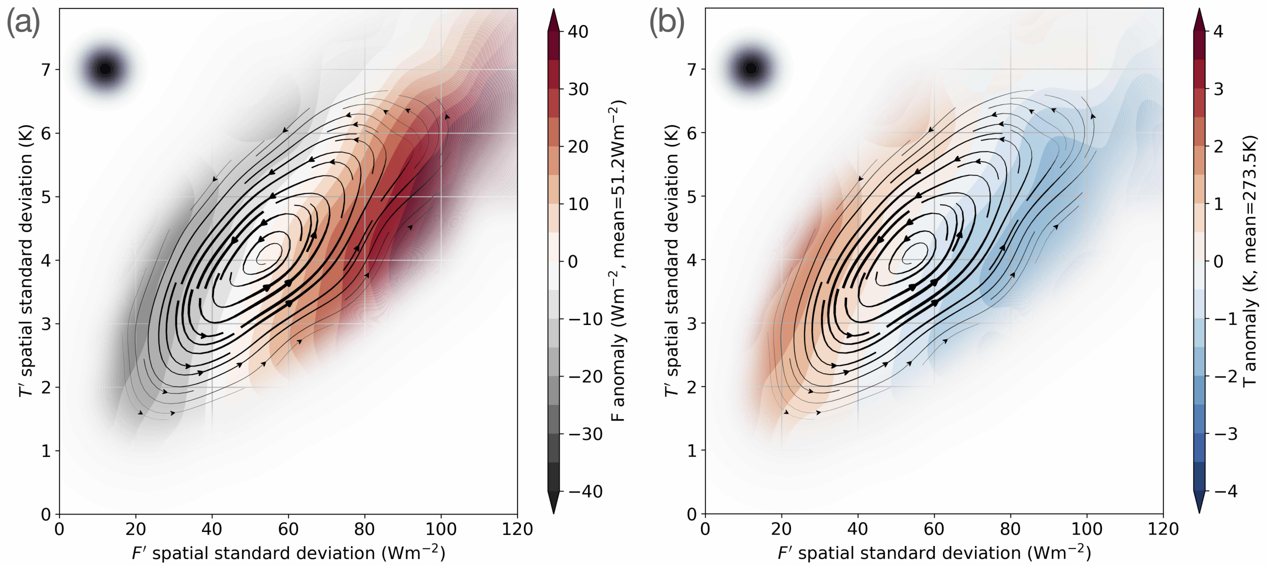

Figure 8. Phase tendencies for spatial-mean F (a) and T (b). Shading represent difference between phase tendency and the mean value of F and T, as reported next to each colour bar. Streamlines as in Fig. 6. The size of the averaging Gaussian filter is indicated by the black-shaded dot in the upper-left corner.

The evolution in time of the potential temperature vertical profiles ~~and climatology~~ along the closed ~~phase space trajectory shown~~ trajectory is portrayed in Fig. 10a, which ~~takes around 5 days to complete.~~shows the difference between the kernel-average and climatology along the closed trajectory shown in Fig. 9. The kernel-averaged mean boundary layer height is also ~~shown by a black solid line.~~ plotted, together with the climatological mean.

The cold and warm phases are characterised respectively by deeper and shallower atmospheric boundary layer. This is ~~consistent~~ compatible with the idea that the growing phase corresponds to the advection of the cold sector into the spatial domain over a warmer SST leading to instability and convective heat fluxes.

~~A downward propagation of the temperature anomalies is also observed, especially in the cooling phase where the temperature anomalies are largest, as the cold sector moves across the spatial domain. The strongest~~ Furthermore, inspecting the time evolution of the anomalous wind direction shown in Fig. 10b, it is found to be consistent with cold air advection in the first half of the cycle, with a north-westerly anomaly backing to a south-easterly wind anomaly and warm air advection in the second half of the cycle. The anomalous wind was computed by removing the climatological mean wind, which is broadly westerly as expected along the storm track.

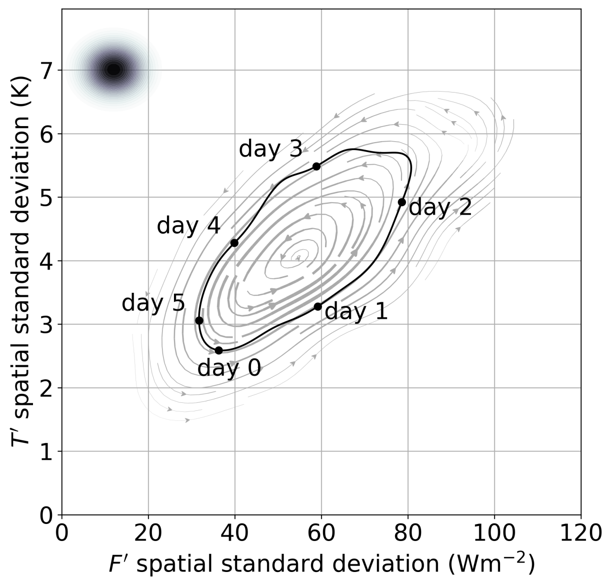

Figure 9. Closed trajectory in the phase space of F' and T' spatial standard deviations chosen for the computation of phase tendencies evolution. Black dots along trajectory indicate time duration in days of each section. The size of the averaging Gaussian filter is indicated by the black-shaded dot in the upper-left corner.

The strongest temperature anomalies are observed in the lower layers of the troposphere, which is symptomatic of the close relationship between the FT index and surface heat exchange, as per definition of the index itself. A tilt in the anomalous temperature profile is observed, especially in the cooling phase where the temperature anomalies are largest, as the cold sector moves across the spatial domain. It is not clear whether this tilt can be related to baroclinic lifecycle. Lim and Wallace (1991) diagnosed a weak forward tilt of temperature also at lower levels, as it must be for growing waves (Hoskins and Heckley, 1981) , though substantially less than the westward tilt of geopotential. The magnitude of the tilt is hard to compare to our results as the x-axis in Fig. 10 maps onto time in a non-trivial way. The stronger tilt/lag of temperature at upper levels that we find is not consistent with observations or expected from theory of idealised life cycles, where in the lower stratosphere at least, the tilt/lag is expected to reverse, as suggested in Lim and Wallace (1991) and Hoskins and Heckley (1981).

The warm phase coincides with a shallower boundary layer, as warm air is advected over the cold side of the SST front, which results in a more stable atmospheric boundary layer and weaker heat exchange. Indeed, the sea surface does not reach temperatures as low as in the preceding cold sector, hence it does not interact as strongly as in the cold phase and this could explain the rapid decay of the heat flux–temperature spatial covariance.

~~These~~ We find that these results are not sensitive to the choice of the specific closed phase space trajectory (not shown).

The heat exchange within a cold sector arguably plays a primary role in driving the FT index. The phase tendency of the area fraction of the spatial domain occupied by the cold sector, shown in Fig. 11, illustrates this further. To estimate the area fraction, we utilise a a diagnostic based upon potential vorticity at the 95kPa level as proposed in a study by Vannière et al. (2016), where it is shown that the cold sector is characterised by a negative potential vorticity signature which proved to be effective as a diagnostic through the comparison with more traditional indicators of the cold sector of extra-tropical weather systems.

In the strengthening phase of the FT index life cycle, the extent of the cold sector almost doubles from about 20% to almost 40% of the domain. This suggests that air–sea heat exchange in the cold sector ~~has~~ may have significant effects on storm evolution, in particular by driving the depletion of the baroclinicity over the domain~~.~~, in accordance with Fig. 5. This appears to be in contradiction with earlier findings in Vannière et al. (2017), where it was suggested that baroclinicity is mainly restored in the cold sector.

Looking at specific events in the FT index, we find that surface heat flux and SST fields are well correlated, especially over warmer sea surfaces. SSTs over the Gulf Stream extension region are indeed characterised by higher spatial variability than air temperatures due to the presence of ~~mesoscale oceanic eddies in~~ both a strong SST front linked to the Gulf Stream and mesoscale oceanic eddies.

Oceanic mesoscale eddies have been shown to play a decisive role in shaping the North Atlantic storm track as they support stronger storm growth rates, making their representation essential for a better description of the storm track (Ma et al., 2017; Zhang et al., 2019). In particular, Foussard et al. (2019) examined the effect of oceanic eddies on storm tracks through an idealised experiment focused on the mid-latitudes, observing a poleward shift of storm trajectories compared to simulations in which mesoscale eddies are removed, as found by Ma et al. (2017) in more realistic simulations for the North Pacific. Foussard et al. (2019) noticed also a larger sensitivity of the atmosphere to positive than to negative anomalies in SST, as the former correspond to a stronger temperature gradient at the air–sea interface.

In light of this, we ~~can~~ conclude that in the FT index growing phase the trigger for heat flux variability corresponds to the advection of (relatively) uniformly cold air masses over the spatially varying SSTs of the Gulf Stream extension region. The strong vertical contrast in temperatures causes enhanced surface heat fluxes which ~~then lead to~~ are then followed by a reaction in the lower atmosphere which experiences a subsequent increase in temperature spatial variability. Despite the SST field changing on much longer timescales, a fixed SST front would therefore still induce heat flux spatial variance on synoptic timescales.

5 Conclusions

Lorenz (1955) showed that diabatic generation of available potential energy is proportional to the covariance between heating and air temperature. ~~This~~ Globally, this term has been estimated to be positive as the residual of momentum and thermodynamic equations and therefore assumed to act as a source of energy for weather systems to feed on. ~~However, using~~ A different picture is observed locally, however. Using data for surface heat fluxes and air temperatures from ERA-Interim, we find that they are

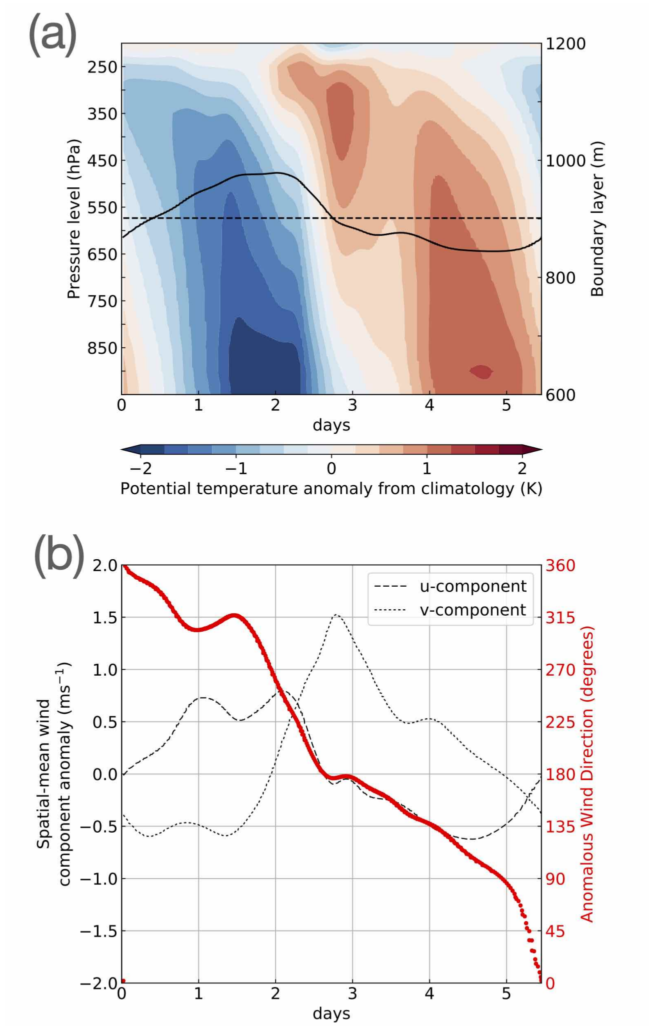

Figure 10. Phase tendency analysis along the closed trajectory shown in Fig. 9 for: (~~b~~a) ~~for~~ area-averaged potential temperature profile (colour shading, difference from winter climatology) and boundary layer height (dashed line, with winter climatological mean indicated by solid line)~~along the closed trajectory shown in panel~~ ; (~~a~~b) meridional (dotted), zonal (dashed) anomalous wind components and corresponding anomalous wind direction (red dots). The horizontal coordinate axis indicates the time progression in days along the closed trajectory~~in days~~.

locally negatively correlated in time and space, in particular upstream of the N. Atlantic storm track, consistent with more recent literature.

~~We~~ In particular, we investigate the heat flux–temperature covariance through the definition of an index (FT index) that measures the local spatial covariance between sensible heat flux and air temperature at 850 hPa. To that effect, a hybrid

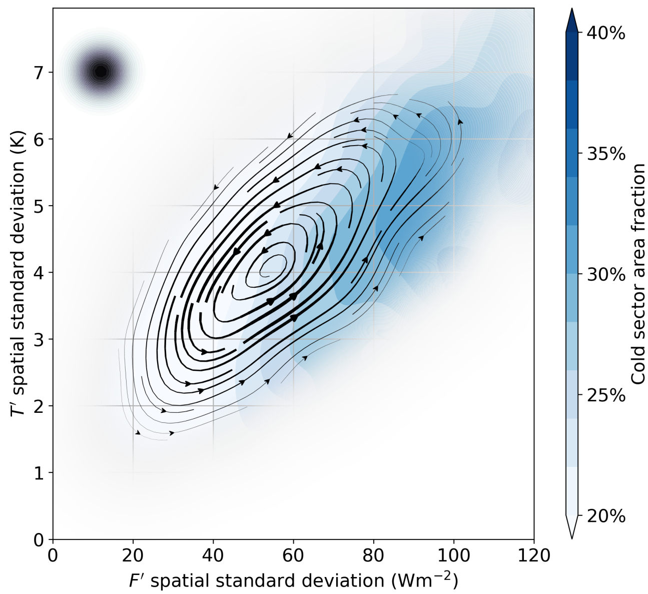

Figure 11. As in Fig. 8, for the phase tendency of cold sector area fraction (percentage of spatial domain occupied by cold sector). The size of the averaging Gaussian filter is indicated by the black-shaded dot in the upper-left corner.

approach was taken where anomalies are defined as deviations from a spatial mean relative to a limited spatial domain, in our case, the Gulf Stream extension region.

The FT index is found to be always negative and characterised by bursts of activity coinciding with strong synoptic storm activity within the spatial domain considered. Composite analysis of strong index values suggest that heat flux-temperature spatial covariance behaves as an energy sink in the evolution of a storm. The peak of the FT index coincides with the ~~start~~ onset of the decaying phase of the storm.~~This is in contrast with global estimates obtained for the Lorenz energy cycle.~~

Heat flux-temperature spatial covariance, as measured by the FT index, and ~~available potential energy~~local baroclinic growth rate, as identified by baroclinicity, are seen to be interacting in a cyclical evolution. Strong FT index values coincide with baroclinicity depletion, while ~~only with~~ a weaker FT index ~~baroclinicity is seen~~ allows the baroclinicity to recover.

Spatial correlation and standard deviations in heat fluxes and air temperatures are observed to be equally important in the build up of strong spatial covariance, with an increase of spatial variability in surface heat fluxes typically preceding an increase for air temperatures spatial variability.

In fact we find, rather counter-intuitively, that the correlation between flux and temperature increases strongly with their variances.

~~The~~ We show that the intensification phase of the FT index coincides with the passage of a storm's cold sector across the region considered~~.~~, which is compatible with the flux variance field shown in Fig. 1. The advection of cold air masses across the meridional ~~sea surface temperature~~ SST gradient and mesoscale oceanic eddies then leads to an increased spatial variability in the surface heat flux field, which ~~eventually bring~~ lead to the FT index to peak values, as heat flux and temperature fields correlate spatially.

Because the FT index is shown to be a good measure of baroclinicity depletion, and peak FT index values are dominated by cold-sector interaction with the spatial SST variance, our results show that the cold sector air-sea fluxes are a thermodynamic sink on the growth potential of storms.

Data availability. In this study we utilised data from ECMWF ERA-Interim, which is freely available from the ECMWF at https://apps.ecmwf.int/datasets/.

Author contributions. AM performed data analyses and prepared the manuscript. MHPA originated the idea for the study, contributed to the interpretation of the results and contributed to the manuscript. We are thankful to both reviewers for their insightful and detailed comments which helped improve the manuscript.

Competing interests. The authors declare that they have no conflict of interest.

Acknowledgements. AM acknowledges PhD studentship funding from the Scenario NERC Doctoral Training Partnership grant NE/R008868/1, co-sponsored by the UK Met Office. The authors thank ECMWF for making their ERA-Interim Reanalysis ~~data~~dataset freely and publicly available.

References

Ambaum, M. H. and Novak, L.: A nonlinear oscillator describing storm track variability, Quarterly Journal of the Royal Meteorological Society, 140, 2680–2684, 2014.

Athanasiadis, P. J. and Ambaum, M. H. P.: Linear Contributions of Different Time Scales to Teleconnectivity, Journal of Climate, 22, 3720–3728, https://doi.org/10.1175/2009JCLI2707.1, https://doi.org/10.1175/2009JCLI2707.1, 2009.

Blackmon, M. L., Wallace, J. M., Lau, N.-C., and Mullen, S. L.: An observational study of the Northern Hemisphere wintertime circulation, Journal of the Atmospheric Sciences, 34, 1040–1053, 1977.

Chang, E. K., Lee, S., and Swanson, K. L.: Storm track dynamics, Journal of climate, 15, 2163–2183, 2002.

Dee, D. P., Uppala, S., Simmons, A., Berrisford, P., Poli, P., Kobayashi, S., Andrae, U., Balmaseda, M., Balsamo, G., Bauer, d. P., et al.: The ERA-Interim reanalysis: Configuration and performance of the data assimilation system, Quarterly Journal of the royal meteorological society, 137, 553–597, 2011.

Foussard, A., Lapeyre, G., and Plougonven, R.: Storm track response to oceanic eddies in idealized atmospheric simulations, Journal of Climate, 32, 445–463, 2019.

Franzke, C., Woollings, T., and Martius, O.: Persistent circulation regimes and preferred regime transitions in the North Atlantic, Journal of the atmospheric sciences, 68, 2809–2825, 2011.

Hoskins, B. and Heckley, W.: Cold and warm fronts in baroclinic waves, Quarterly Journal of the Royal Meteorological Society, 107, 79–90, 1981.

Hoskins, B. and Hodges, K.: New perspectives on the Northern Hemisphere winter storm tracks, Journal of the Atmospheric Sciences, 59, 1041–1061, 2002.

Hoskins, B. J. and Valdes, P. J.: On the existence of storm-tracks, Journal of the atmospheric sciences, 47, 1854–1864, 1990.

Hoskins, B. J., James, I. N., and White, G. H.: The shape, propagation and mean-flow interaction of large-scale weather systems, Journal of the atmospheric sciences, 40, 1595–1612, 1983.

Hotta, D. and Nakamura, H.: On the significance of the sensible heat supply from the ocean in the maintenance of the mean baroclinicity along storm tracks, Journal of climate, 24, 3377–3401, 2011.

James, I. N.: Introduction to circulating atmospheres, Cambridge University Press, 1995.

Li, L., Ingersoll, A. P., Jiang, X., Feldman, D., and Yung, Y. L.: Lorenz energy cycle of the global atmosphere based on reanalysis datasets, Geophysical Research Letters, 34, 2007.

Lim, G. H. and Wallace, J. M.: Structure and evolution of baroclinic waves as inferred from regression analysis, Journal of the atmospheric sciences, 48, 1718–1732, 1991.

Lorenz, E. N.: Available potential energy and the maintenance of the general circulation, Tellus, 7, 157–167, 1955.

Ma, X., Chang, P., Saravanan, R., Montuoro, R., Nakamura, H., Wu, D., Lin, X., and Wu, L.: Importance of resolving Kuroshio front and eddy influence in simulating the North Pacific storm track, Journal of Climate, 30, 1861–1880, 2017.

Marques, C. A., Rocha, A., Corte-Real, J., Castanheira, J. M., Ferreira, J., and Melo-Gonçalves, P.: Global atmospheric energetics from NCEP–Reanalysis 2 and ECMWF–ERA40 Reanalysis, International Journal of Climatology: A Journal of the Royal Meteorological Society, 29, 159–174, 2009.

Messori, G. and Czaja, A.: On the sporadic nature of meridional heat transport by transient eddies, Quarterly Journal of the Royal Meteorological Society, 139, 999–1008, https://doi.org/10.1002/qj.2011, https://rmets.onlinelibrary.wiley.com/doi/abs/10.1002/qj.2011, 2013a.

Messori, G. and Czaja, A.: On the sporadic nature of meridional heat transport by transient eddies, Quarterly Journal of the Royal Meteorological Society, 139, 999–1008, 2013b.

Nakamura, H., Sampe, T., Goto, A., Ohfuchi, W., and Xie, S.-P.: On the importance of midlatitude oceanic frontal zones for the mean state and dominant variability in the tropospheric circulation, Geophysical Research Letters, 35, 2008.

Novak, L., Ambaum, M. H., and Tailleux, R.: The life cycle of the North Atlantic storm track, Journal of the Atmospheric Sciences, 72, 821–833, 2015.

Novak, L., Ambaum, M., and Tailleux, R.: Marginal stability and predator–prey behaviour within storm tracks, Quarterly Journal of the Royal Meteorological Society, 143, 1421–1433, 2017.

Oort, A. H.: On estimates of the atmospheric energy cycle, Mo. Wea. Rev, 92, 1964.

Oort, A. H. and Peixoto, J. P.: The annual cycle of the energetics of the atmosphere on a planetary scale, Journal of Geophysical Research, 79, 2705–2719, 1974.

Orlanski, I.: Bifurcation in eddy life cycles: Implications for storm track variability, Journal of the atmospheric sciences, 60, 993–1023, 2003.

Peixoto, J. P. and Oort, A. H.: Physics of climate, New York, NY (United States); American Institute of Physics, 1992.

Rivière, G.: Effect of latitudinal variations in low-level baroclinicity on eddy life cycles and upper-tropospheric wave-breaking processes, Journal of the Atmospheric Sciences, 66, 1569–1592, 2009.

Swanson, K. L. and Pierrehumbert, R. T.: Lower-tropospheric heat transport in the Pacific storm track, Journal of the atmospheric sciences, 54, 1533–1543, 1997.

Ulbrich, U. and Speth, P.: The global energy cycle of stationary and transient atmospheric waves: results from ECMWF analyses, Meteorology and Atmospheric Physics, 45, 125–138, 1991.

Vannière, B., Czaja, A., Dacre, H., Woollings, T., and Parfitt, R.: A potential vorticity signature for the cold sector of winter extratropical cyclones, Quarterly Journal of the Royal Meteorological Society, 142, 432–442, 2016.

Vannière, B., Czaja, A., and Dacre, H. F.: Contribution of the cold sector of extratropical cyclones to mean state features over the Gulf Stream in winter, Quarterly Journal of the Royal Meteorological Society, 143, 1990–2000, 2017.

Zhang, X., Ma, X., and Wu, L.: Effect of Mesoscale Oceanic Eddies on Extratropical Cyclogenesis: a Tracking Approach, Journal of Geophysical Research: Atmospheres, 2019.